Mascle, J., Lohmann, G.P., and Moullade, M. (Eds.), 1998
Proceedings of the Ocean Drilling Program, Scientific Results, Vol. 159

7. THERMAL DIAGENESIS OF CRETACEOUS SEDIMENT RECOVERED AT THE CÔTE D'IVOIRE–GHANA TRANSFORM MARGIN[1]

Mary Anne Holmes[2]

ABSTRACT

The early opening of the South Atlantic ocean along the eastern Romanche Fracture Zone, including an initial phase of transform faulting and pull-apart basin formation, followed by the generation of a seafloor spreading center, was investigated during Ocean Drilling Program Leg 159 to the Côte d'Ivoire-Ghana continental margin. Clay minerals in the <0.5-µm fraction of tectonically disturbed sediment recovered during this leg were analyzed by X-ray diffraction to determine the extent of thermal diagenesis caused by the passing of the South Atlantic spreading center along this transform margin, and to date the passing. Results from Sites 959-961 reveal mild thermal alteration of clays, to paleotemperatures of 120°–170°C, in older, mostly undated sediment, in response to an elevated paleogeothermal gradient, as indicated by the absence of randomly interstratified illite/smectite group clays (R = 0 I/S clay), and the presence of dominant regularly interstratified (R = 1) I/S clay. Thermally altered sediment at these sites underlie unaltered sediment with likely erosional contacts. Based on a date of nannofossil biozone CC9b for the oldest unaltered sediment at Site 959, the thermal event there must have been pre-CC9b.

At Site 962, drilled on a minor marginal ridge to the west of Sites 959–961, heat has altered clay in basal sediment to R = 1 I/S, and the transition uphole to thermally unaltered sediment, bearing R = 0 I/S clay, was recovered over a 175-m-thick interval, indicating the thermal event was intense but short-lived. Near-vertical beds at the top of the mid-Cretaceous section were not heated, while folded and unfolded sediments, 175 m deeper, were heated. Based on estimations of paleotemperatures of these sediments, a paleogeothermal gradient of near 350°C/km would be required to form the observed clay mineral assemblages. This heating must postdate the age of the sediments, which is latest Albian–Cenomanian (nannofossil biozone CC9b). Thus, the spreading center passed between Sites 959/960 and Site 962 sometime during the latest Albian–Cenomanian.

INTRODUCTION

Ocean Drilling Program (ODP) Leg 159 sailed to the Côte d'Ivoire-Ghana continental margin to investigate the nature and timing of the opening of this part of the equatorial Atlantic Ocean, an area known to be affected by transform faulting along the Romanche and Saint Paul Fracture Zones (Fig. 1; Shipboard Scientific Party, 1996a). Specifically, we went to test the hypothesis that rifting began with a stage of intra-continental transform faulting and formation and fill of extensional basins. This phase was followed by the formation of an active oceanic spreading center, which passed by the transform margin and caused uplift and heating of accumulated sediment. One of the extensional or pull-apart basins is now the Deep Ivorian Basin (Figs. 1, 2). It is bounded to the south by uplifted sediment which formed a marginal ridge, the Côte d'Ivoire-Ghana marginal ridge, during the passage of the active rift zone. Three Sites, 959, 960, and 961, were drilled on the Côte d'Ivoire-Ghana marginal ridge, where it was thought that older sediment would be more accessible. Time permitted drilling a fourth site, 962, on an adjacent marginal ridge to the west (Fig. 2).

The age of the opening of the fracture zone is thought to be Early Cretaceous based on two mid through late Albian samples of siliciclastic sediment taken during dives and while drilling along the marginal ridge (Mascle et al., 1996). Ambiguity of the stratigraphic position of these samples, that is, whether they are from syn- or postrift strata, left the actual date of the opening in this region uncertain. The continental margin was thought to pass the oceanic spreading center either during the mid-late Albian (i.e., the age of the samples) or pre–mid-Albian (i.e., older than the samples). When it passed, it may have caused high heat flow and induced anchizone or higher grade metamorphism of syntransform sediment (Mascle et al., 1996).

Tectonically disturbed sediment was recovered at all four sites drilled during Leg 159. Disturbance of the sediment is evident from its greater induration compared to overlying Maastrichtian and younger sediment, its folding, normal and reverse faulting, flower structures, and poor recovery. Samples were taken for the present study from the deeper parts of the sediment column in order to learn the nature and extent of thermal diagenesis of the sediment. In particular, clays were extracted and examined for their degree of thermal diagenesis. Clay minerals, particularly those formed during subaerial weathering, become increasingly unstable with increased burial depth (for reviews, see Eslinger and Pevear, 1988; Velde, 1985; Pollastro, 1993), and temperature is believed to play a more important role than pressure (e.g., Elliott and Matisoff, 1996). Other factors that control clay mineral transformations at increased temperatures and pressures include original sediment composition, porosity, permeability, potassium concentration of the pore waters, and time. Smectite group minerals are perhaps the most unstable phyllosilicate clay mineral as burial depth increases and/or temperatures of sediment rise. The mineralogic changes it undergoes in the smectite to illite reaction are identifiable by X-ray diffraction (XRD; see Reynolds, 1980; Moore and Reynolds, 1989). The reaction shows that smectite becomes increasingly nonexpandable through temperatures up to about 100°C (Hoffman and Hower, 1979; Pollastro, 1993), and the nonexpandable layers appear, or are added, randomly through the mineral lattice. Randomly interstratified illite/smectite contains 0%–60% nonexpandable layers and is assigned the Reichweite ("reach back"), or R-value of 0 (Reynolds, 1980), designated R = 0 I/S clay (Pollastro, 1993). Above a temperature range of 100°–140°C, a regularly interstratified illite/smectite appears. It contains 60%–90% nonexpandable layers and is assigned the Reichweite value of 1, designated R = 1 I/S clay. At temperatures above 170°–180°C, regularly interstratified clay generally has fewer than 10% nonexpandable layers, the Reichweite value is 3, and is designated R = 3 I/S clay.

[1]Mascle, J., Lohmann, G.P., and Moullade, M. (Eds.), 1998. *Proc. ODP, Sci. Results*, 159: College Station, TX (Ocean Drilling Program).

[2]Department of Geology, 214 Bessey Hall, University of Nebraska-Lincoln, Lincoln, NE 68588-0340, U.S.A. mholmes@unlinfo.unl.edu

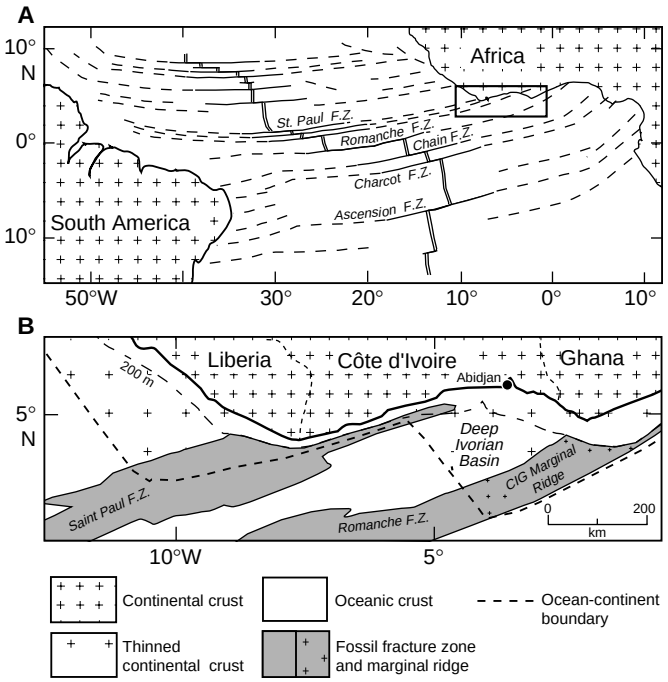

Figure 1. **A.** Location of study area along the Côte d'Ivoire-Ghana margin. **B.** Inset of A showing structural elements in the region of ODP Leg 159. CIG = Côte d'Ivoire-Ghana Marginal Ridge, where Sites 959–960 are located. From Mascle et al. (1996).

Shipboard examination revealed the presence of I/S clay in tectonically disturbed sediment at depth from all four sites from Leg 159. This study reports on the results of XRD studies on the fine clay (<0.5 µm) fraction to determine what the extent of clay mineral diagenesis might contribute to our understanding of the evolution of this transform-passive continental margin.

LITHOLOGIES

Site 959

Sediment that has been subject to deformation and possible heating was recovered at the base of several holes (Fig. 3). The first site drilled, Site 959, is located on the southern edge of the Deep Ivorian Basin, on the northern flank of the Côte d'Ivoire-Ghana Marginal Ridge (Fig. 2). In Hole 959D, relatively undisturbed black clay- and siltstones of Late Cretaceous through early Paleocene age (lithologic Unit III; Pl. 1, Fig. 1) overlie early Coniacian to late Albian mixed siliceous and carbonate clastics (lithologic Unit IV; Pl. 1, Fig. 2), which in turn overlie disturbed quartz sandstone and silty claystone of unknown age (lithologic Unit V; Fig. 4; Pl. 2, Figs. 1–4; Shipboard Scientific Party, 1996b). The 231–m-thick lithologic Unit III of laminated to faintly bioturbated black clay- and siltstones, dips increasingly downhole from near level at the top of the section to values of 20°–30° between 960 and 1000 meters below seafloor (mbsf; Shipboard Scientific Party, 1996b). Rare to common burrows are replaced by pyrite and/or barite and show slightly asymmetric pressure shadows (Pl. 1, Fig. 1; Shipboard Scientific Party, 1996b). Some of the laminae show concentrations of glauconite, pyrite and barite, suggesting that mineralization was syndepositional and that the bottom sediment was sometimes reworked. Star-shaped kaolin pods and thin (2- to 4-mm-wide) veins occur between 995.4–1010.5 mbsf (Sections 159-959D-62R-1 and 2 and 159-959D-63R-2 and 4). Phosphate nodules, some reworked into graded beds and others apparently in situ, occur near the base of the section.

The contact between the black clay- and siltstones and the underlying mixed siliceous-carbonate unit was not recovered, and the mixed siliceous/carbonate clastics of lithologic Unit IV were poorly recovered over a 38.4-m-thick interval. It contains graded beds of quartz, shell fragments, and dolomite rhomb sand, suggesting redeposition from a reef bearing red algae and mollusks (Pl. 1, Fig. 2; Shipboard Scientific Party, 1996b). A few thin veins of barite occur sporadically through this unit. The basal lithologic Unit, V, is moderately to severely deformed, with beds dipping from near 0° to near 90° (Shipboard Scientific Party, 1996b). The uppermost core included in this unit, Core 159-959D-71R, is distinctly different from the sediment in the underlying cores by being massive and containing numerous water-escape structures (Pl. 2, Figs. 1–3). Sheet structures and sand dikes are common (Pl. 2, Figs. 2, 3). This sand also contains thin, anastomozing veins filled with a gray mineral (Pl. 2, Fig. 2), The sand in the underlying cores, by contrast, is graded or finely laminated, strongly dipping and in some intervals, brecciated (Pl. 2, Fig. 4). Small veins in Core 159-959D-73R are filled with kaolin (based on shipboard XRD) and calcite. The sediment of Core 159-959D-71R is distinct from that of the overlying cores, as well. It is a different color (gray, N6 to N7 vs. olive gray, 10Y 3/1–5/1 for Core 159-959D-67R), is massive (vs. laminated to distinctly bioturbated) with no signs of bioturbation, and contains no calcareous material. This core probably forms a separate subunit of lithologic Unit V.

Site 960

Site 960 is on the top of the Côte d'Ivoire-Ghana Marginal Ridge, three mi south of Site 959 (Fig. 2). Tertiary sediment at this site is underlain by highly condensed, partly calcareous, partly phosphatized upper Turonian–upper Coniacian age sediment (Fig. 3; Pl. 3, Fig. 1), lithologic Subunit IVA, (Fig. 5; see Watkins, et al., Chap. 26, this volume). These in turn overlie 145 m of late Turonian–late Coniacian mixed carbonate-siliciclastic sediment, lithologic Subunit IVB, probably redeposited from a shallow-water carbonate environment (Fig. 3; Pl. 3, Fig. 2; Shipboard Scientific Party, 1996c; see Marcano et al., Chap. 8, this volume). Beneath lithologic Unit IV, 122 m of deformed micritic silty sandstones, sideritic siltstones, and silty claystone was recovered to the base of Hole 960A (Fig. 5; Pl. 3, Figs. 2–4). This section comprises two distinct lithologic subunits. An upper one, lithologic Subunit VA, is similar to lithologic Unit V in Hole 959D, comprising massive to laminated or wavy-laminated fine sandstone and siltstone (Pl. 3, Fig. 4). Other structures include asymmetrical ripples, convolute beds and water-escape structures (Pl. 3, Fig. 3). Organic C content is as high as 2.1%, and both siderite and pyrite are common (Shipboard Scientific Party, 1996c). This subunit is interpreted as shallow marine, probably deltaic (Shipboard Scientific Party, 1996c). Parts of this subunit have been intensely brecciated and deformed, and in some places apparently overturned (Shipboard Scientific Party, 1996c). Veining and fractures, many filled with calcite or a kaolin clay, are common.

The underlying Subunit VB, is distinctly different in that it displays very fine laminations alternating with graded beds that bear a variety of sole marks, particularly scour-and-fill and ball-and-pillow structures (Pl. 4, Fig. 1). Over some intervals, these beds grade upward from massive sand through rippled to laminated sand and silt, and are interpreted as turbiditic in origin (Shipboard Scientific Party, 1996c; Pl. 4, Fig. 1). The subunit is interpreted as lacustrine, owing to the bedforms and the absence of pyrite, formed in a pull-apart basin during transtensional motion (Shipboard Scientific Party, 1996c). The contact between the relatively undisturbed, Upper Cretaceous lithologic Unit IV and the highly deformed, undated lithologic Unit V was disturbed by drilling but apparently was comprised of an unconsolidated mud (Pl. 3, Fig. 2). As lithologic Subunit VA is interpreted as a shallow marine (probably deltaic) deposit, the drilling-disturbed contact between lithologic Units IV and V was sampled for this study to determine if any subaerial weathering occurred during

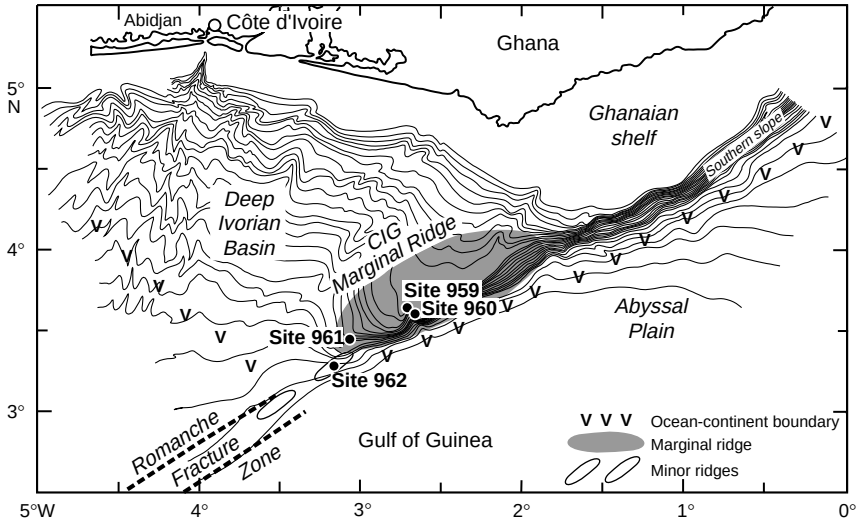

Figure 2. Location of ODP drill Sites 959-961 on the Côte d'Ivoire-Ghana Marginal Ridge, and of Site 962 on a westward, minor ridge. From Mascle et al. (1996).

the hiatus between deposition of the deformed and undeformed units. Structural deformation of the lacustrine subunit (Subunit IVB) is identical to the one overlying it (Subunit IVA), including numerous normal and reverse microfaults, pop-up structures, intense brecciation, fractures filled by calcite, pyrite, kaolin, or rare barite (Shipboard Scientific Party, 1996c). Kaolin veins cluster in Cores 159-960A-40R through 46R, where they are thin, sigmoidal, or have en echelon patterns suggesting tensional stress during or after formation (Shipboard Scientific Party, 1996c).

Site 961

Site 961 is located at the westernmost expression of the marginal ridge (Fig. 2). The pelagic Tertiary section is underlain by the deformed siliciclastic lithologic Unit III (Figs. 3, 6). The age of lithologic Unit III is uncertain, ranging from perhaps Bajocian to Maastrichtian age, based on calcareous nannofossils (see Watkins et al., Chap. 26, this volume). Bedforms and sediment composition are fairly uniform, but core recovery was poor over both the 120-m-thick section recovered from Hole 961A and the 158-m-thick section recovered from Hole 961B (Fig. 6; Shipboard Scientific Party, 1996d). Beds of sand to clayey siltstone in this unit are massive or are lenticularly laminated, with rare convolute bedding. The overall fine grain size, the uniformity of the section, and the presence of rare nannofossils and hummocky cross beds suggest deposition on an outer shelf that experienced periodic reworking by waves, probably an offshore equivalent of the deltaic sediment recovered at Site 960 (Shipboard Scientific Party, 1996c). Tectonic disturbance is indicated by the presence of breccia, slickensided fractures, fractures filled by calcite, normal microfaults, near-vertical bedding, and rough crenulation interpreted as incipient cleavage (Pl. 4, Fig. 2; Shipboard Scientific Party, 1996d). Kaolin-filled veins occur in Section 159-961B-5R-1.

Site 962

Site 962 is located on a separate ridge to the west of Sites 959–961 (Fig. 2). Deformed sediment of Late Albian (and possibly older) age, lithologic Unit III (Pl. 4, Figs. 3, 4), underlies an abbreviated Tertiary and mid-Cretaceous pelagic section (Fig. 3). In Hole 962D, 270 m of redeposited siliciclastic and calciclastic sediment was recovered (Fig. 7; Shipboard Scientific Party, 1996e). Claystones are massive or laminated with silt or sand, and contain abundant nannofossils in some intervals (Pl. 4, Fig. 4), abundant dolomite in others. Sand- and siltstones are laminated- to lenticular-bedded, or in some intervals, graded, with locally abundant dolomite rhombs. The limestones are composed of sparry and micritic calcite, with benthic and planktonic foraminifers. They also commonly contain quartz sand and silt, and, in some intervals, abundant dolomite. They are usually laminated, with the laminae commonly cut by scours or topped by isolated ripples (Shipboard Scientific Party, 1996e). Tectonic disturbance is evident from beds dipping to nearly vertical (Pl. 4, Fig. 3), brecciated zones, faults and fracturing, which reduced core recovery, and ubiquitous veins filled with calcite, some of which also contain pyrite (Shipboard Scientific Party, 1996e).

METHODS

One hundred thirty two samples were taken of sediment from the deeper parts of each hole, with preference given to the finer grained (i.e., clay-rich) sediment. Samples were washed with distilled water and dispersed in sodium hexametaphosphate solution, treated with ultrasound for 3–4 min, and centrifuged to remove the <0.5-µm fraction (Jackson, 1975). The supernatant was decanted into a Milipore filtration apparatus and an oriented mount prepared after the method of Drever (1973). Kaolin veins were scraped with stainless steel dental tools and examined as random mounts by XRD. The kaolin polytype was identified according to peak positions between 23° and 57°2θ, as given in Moore and Reynolds (1989).

Samples were X-rayed on a Scintag PAD V X-ray diffractometer equipped with a graphite monochromator, and 0.67° and 0.76° divergence slits on either side of a collimator. Oriented samples were scanned from 2° to 45°2θ in the air-dried state, from 2° to 30°2θ after ethylene glycol solvation (60°C over ethylene glycol vapor in a desiccator overnight), and from 2° to 10°2θ after heating selected samples to 350°C for 1 hr in a muffle furnace. Peak areas and positions were calculated from the glycolated scans using the split Pearson model (unweighted peaks) in the Profile Fitting package of Scintag's DMS software (v. 3.1).

Mineral identification followed standard methods. Kaolinite and chlorite were distinguished by the slow scan method of Biscaye (1964) over the 004 peak of chlorite and the 002 peak of kaolinite. Where these peaks were too small to allow an accurate position, the 002 peak of chlorite and the 001 peak of kaolinite were used. This assumes that a peak position of 7.10 Å indicates chlorite and 7.16 Å indicates kaolinite (Biscaye, 1964). Illite and mixed-layer clays were identified from diffractograms of samples treated with ethylene glycol by referring to Reynolds (1980), Moore and Reynolds (1989), and the Δ2θ method of Srodon (1980). In addition, diffractograms of glycolated samples were compared visually to those generated by NEWMOD (Reynolds, 1985). In brief, for glycolated samples, any peak at 16–17 Å was identified as R = 0 I/S clay, a peak near 12–13 Å as R

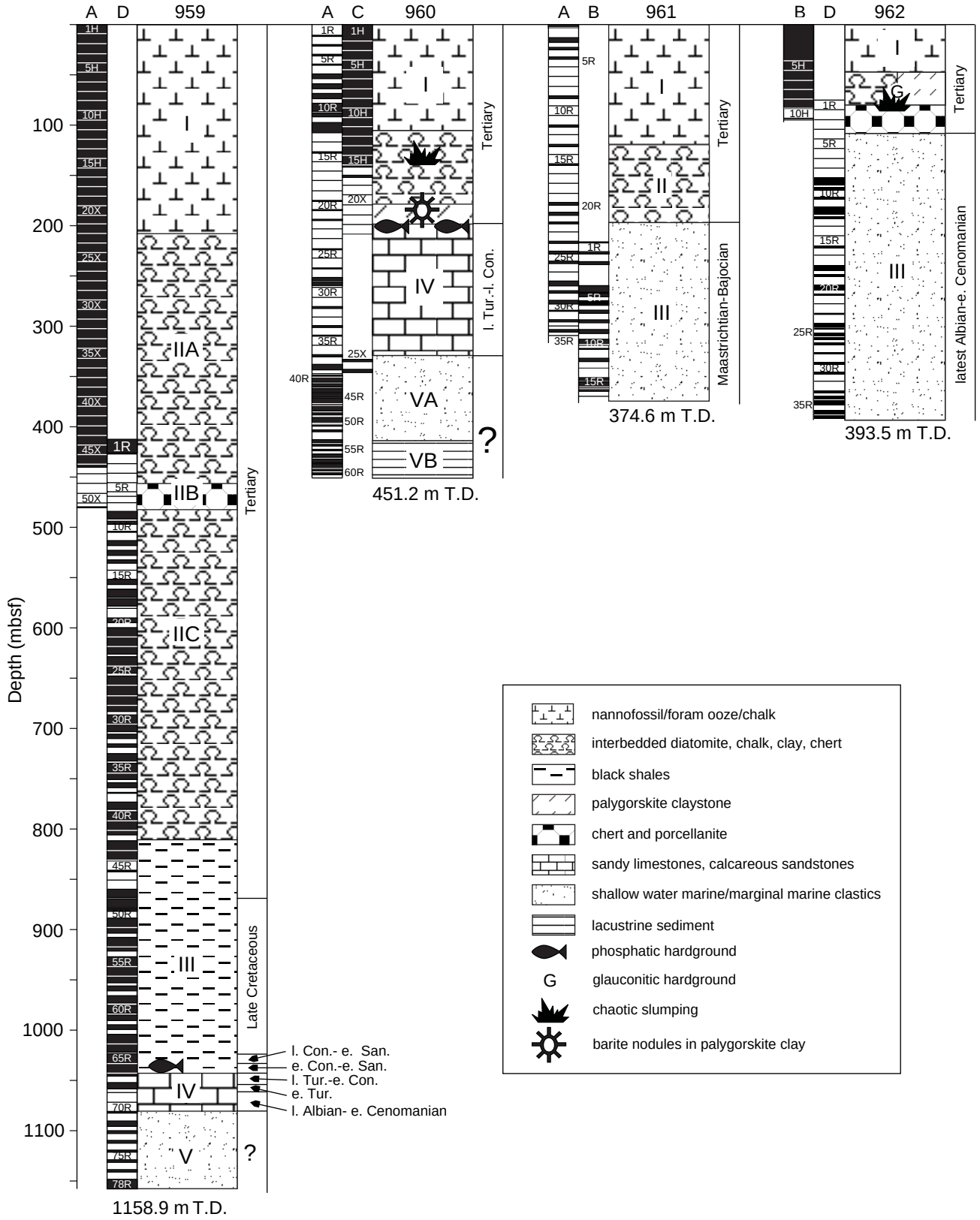

Figure 3. Summary of lithologic units from all four sites, ODP Leg 159. Letters at tops of columns refer to drill holes. Blackened columns to left of lithologies indicate where cores were taken and the percent recovery. Depth, mbsf, in meters below seafloor. T.D. = total depth. Roman numerals refer to shipboard-defined lithologic units. For ages, l. = late; e. = early; C and Con. = Coniacian; San. = Santonian; T and Tur. = Turonian; Cen. = Cenomanian. Dates for Cretaceous from Watkins, et al., Chap. 26, this volume.

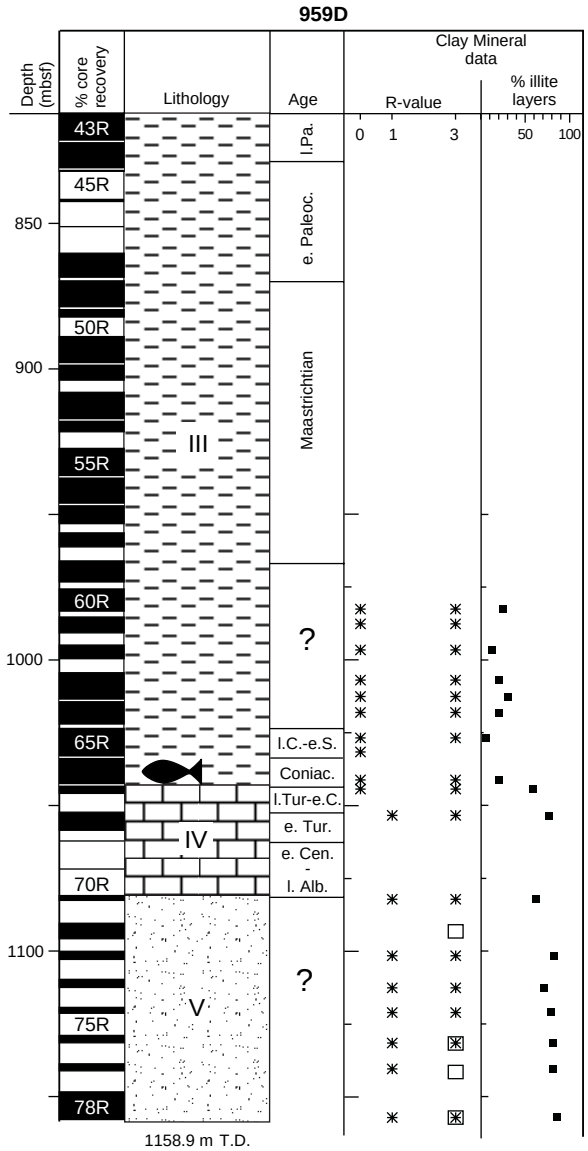

Figure 4. Summary of XRD data on the <0.5-µm-sized fraction from Hole 959D. For key to lithologic symbols, see Figure 3. R-value = Reichweite value; open squares = data on the <2-µm-sized fraction, from T. Pletsch (pers. comm., 1996); l. = late; e. = early; Pa. = Paleocene; C. = Coniancian; S. = Santonian; Coniac. = Coniacian; Tur. = Turonian; Cen. = Cenomanian.

= 1 I/S clay, and a low-angle shoulder on the 10 Å illite peak near 11 Å as R = 3 I/S clay. In addition, peak positions for 002/003 I/S peaks between 15° sand 20°2θ were calculated using the profile-fitting software. A peak at 5.0 Å was used to identify the presence of illite where no 11 Å shoulder occurred on the 10 Å peak. Had a shoulder appeared, this peak might indicate R = 3 I/S clay. Peaks between 5.0 and 5.3 Å were identified as R = 1 I/S clay, and peaks between 5.4 and 5.7 Å were identified as R = 1 I/S clay. Where possible, the presence of both 001/002 and 002/003 I/S peak positions were used to obtain a °Δ2θ value (Srodon, 1980), from which percent of nonexpandable layers was calculated from values published in Moore and Reynolds (1989).

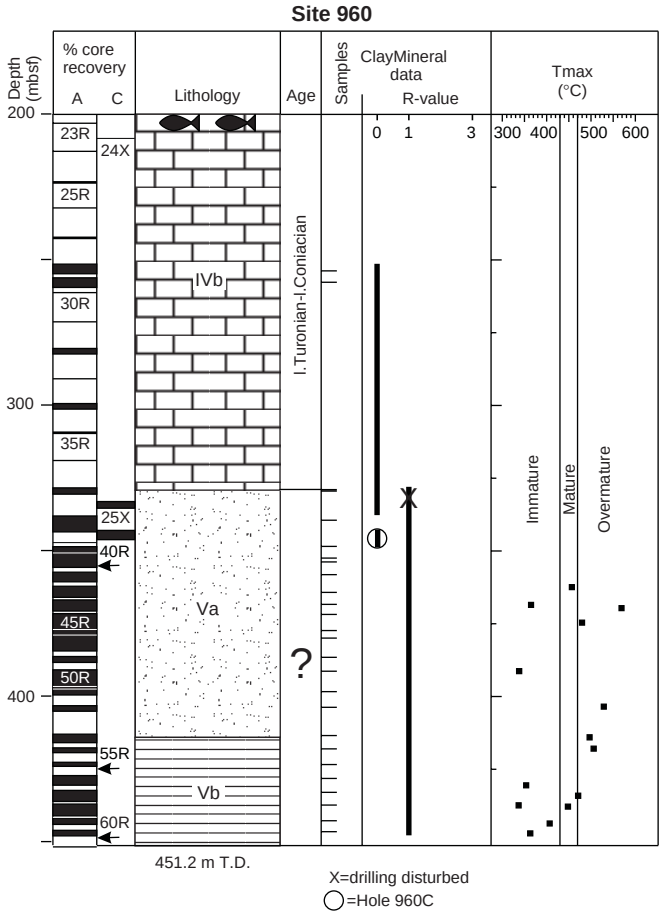

Figure 5. Summary of XRD data on the <0.5-µm-sized fraction from Holes 960A and 960C. Fish represent phosphatic hardgrounds of lithologic Subunit IVA. For key to lithologic symbols, see Figure 3. T_{max} data from Shipboard Scientific Party (1996b).

RESULTS

Site 959

Samples from the base of the black clay- and siltstones of lithologic Unit III were examined and found to contain predominantly R = 0 I/S clay (randomly interstratified illite/smectite mixed-layer clay), with 5%–30% nonexpandable (illite) layers (Figs. 4, 8A; Table 1). There is no trend of increased nonexpandability with depth within lithologic Unit III over the interval examined (982.7 to 1041.4 mbsf). A small amount of highly illitic I/S (R = 3) occurs in samples from Cores 159-959D-62R through 63R, and a small amount of illite mixed with R = 3 I/S clay occurs in samples from Cores 159-959D-64R through 66R. Both 10 and 5 Å peaks of illite are quite sharp and less asymmetrical in the <2-µm fraction, suggesting the presence of detrital mica in the coarser fraction. Traces of chlorite are present in three samples from 1018.2, 1026.9, and 1041.4 mbsf (Table 1), and a trace of kaolinite occurs in one sample (Sample 159-959D-64R-3, 48–50 cm; 1018.2 mbsf). Trace amounts of detrital quartz, as indicated by the greater height of the 3.34 Å peak relative to the 4.26 Å peak (Eslinger et al., 1973), were found in all but two samples (996.7 and 1007.1 mbsf). Traces of calcite occur in the three lowermost samples

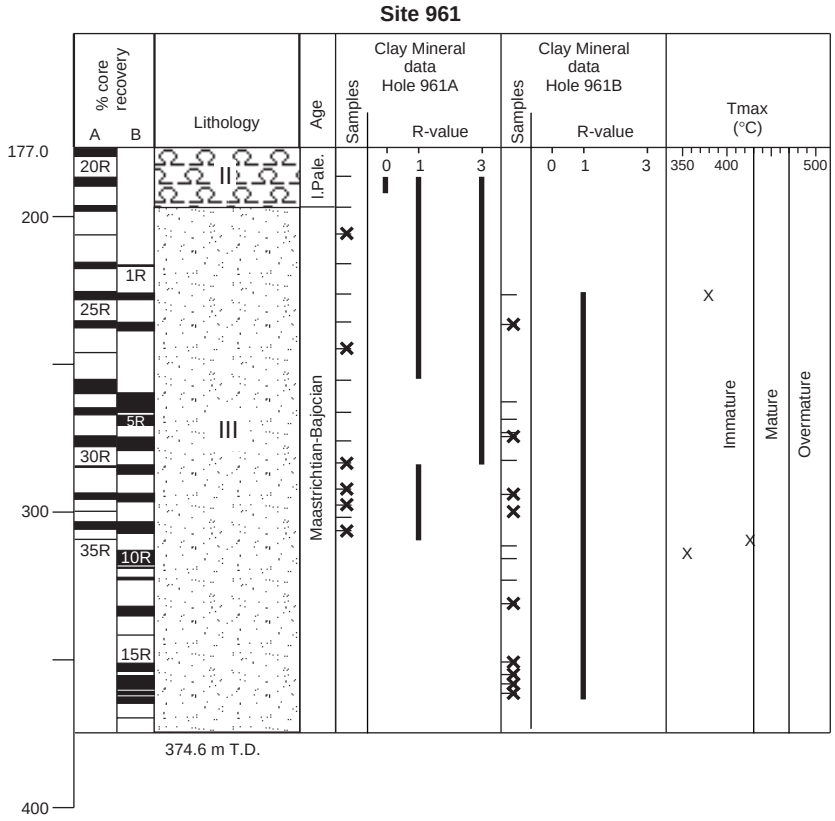

Figure 6. Summary of XRD data on the <0.5-µm-sized fraction from Holes 961A and 961B. For key to lithologic symbols, see Figure 3. X over sample locality indicates an intact sample. T_{max} data from Shipboard Scientific Party (1996c).

and at 987.8 mbsf. A trace of plagioclase and potassium feldspar occur in samples from 1007.1 and 1026.9 mbsf, respectively.

Random interstratification of the clay persists downhole to the top of lithologic Unit IV (Sample 159-959D-67R-1, 118–121 cm; 1044.5 mbsf), but the proportion of nonexpandable layers is greatly increased, to 58% (Table 1). Detrital illite is again present, as indicated by peaks at both 10 and 5 Å. A trace of a 7 Å mineral is present and appears to be kaolinite with no chlorite present, based on the absence of both a 14 and a 4.7 Å peak. The 002 kaolinite/004 chlorite peaks near 25°2θ were too small to be distinguished from the background. A trace of detrital quartz is also present. The next downhole sample from lithologic Subunit IVA, which occurs 9.1 m deeper (Sample 159-959-68R-1, 57–60 cm; 1053.6 mbsf), contains no R = 0 I/S clay, but only R = 1 I/S clay, with 76% illite layers, as indicated by the presence of a broad 10.8 Å peak in the air-dried sample, which splits into two peaks, one at 13.8 Å and the other at 9.56 Å, upon glycolation (Fig. 8B). Illite or an R = 3 clay is also present, as indicated by a broad, asymmetrical peak at 10 Å and a peak at 5 Å. In the <2-µm fraction, the 10 Å peak is quite sharp, again suggesting detrital mica. In addition, there are traces of chlorite, kaolinite, quartz and calcite in the <0.5-µm fraction (Table 1). The next sample examined is 28.7 m deeper (Sample 159-959D-71R-1, 64–67 cm; 1082.3 mbsf) and contains R = 1 I/S clay with 62% nonexpandable layers, as indicated by a superlattice peak at 24.3 and a peak at 13.3 Å in the air-dried state that shifted to 27.8 and 11.2 Å in the glycolated sample (Fig. 8C). 10 and 5 Å peaks are again present, indicating illite. Chlorite is also present. The last five samples from 1101.8 to 1157.3 mbsf all contain R = 1 I/S clay with 70%–85% nonexpandable layers. Expandability decreases with increased depth over this 55.5 m interval. Chlorite and detrital illite are present in all of these samples, and the lower two also contain a trace of kaolinite (Table 1; Fig. 8D–E).

Site 960

A white kaolin vein, prepared as a random mount, has peak positions that indicate the presence of minor kaolinite and dominant nacrite, a polytype of kaolinite (Fig. 9A). Two samples from lithologic Subunit IVB contain R = 0 I/S clay, illite, kaolinite, and calcite (Table 2; Fig. 5). The upper sample also contains R = 3 I/S clay (Fig. 9B). Below the unconformable contact, all samples contain R = 1 I/S clay, with traces of R = 3 I/S clay in three samples (at 413.4, 418.0, and 428.2 mbsf; Figs. 5, 9C). Chlorite is also present in all samples, as is illite. The chlorite polytype is either Ia or Ib (β = 90°; Hayes, 1970). Kaolinite and quartz are present in most samples (Table 2). Samples from all overlying, Tertiary lithologic units contain a highly expandable R = 0 I/S clay, with varying amounts of illite and kaolinite. A sample from the deepest core of Hole 960C, Sample 159-960C-26X-CC, 4–6 cm, contains R = 0 I/S clay, with 25% expandable layers (Fig. 9D). Illite and traces of kaolinite, calcite and quartz are also present. These samples correspond lithologically to lithologic Unit IV, based on smear-slide observations.

Site 961

Sample 159-961A-21R-2, 82–85 cm, contains a mixture of R = 0, R = 1, and R = 3 I/S clay (Figs. 6, 10A). The samples below it in Hole 961A and all of the samples in Hole 961B contain no R = 0 I/S clay (Table 3; Fig. 6). Drilling recovery was very poor in both holes, and many of the samples are from drilling-induced breccia, possibly representing a mix from different depths in the hole. Samples from intact, whole-round samples of the core are indicated on the figures. R = 1 I/S clay dominates in the sediment of both holes. R = 3 I/S clay, identified as a distinctive ~11 Å shoulder on a 10 Å peak in glycolat-

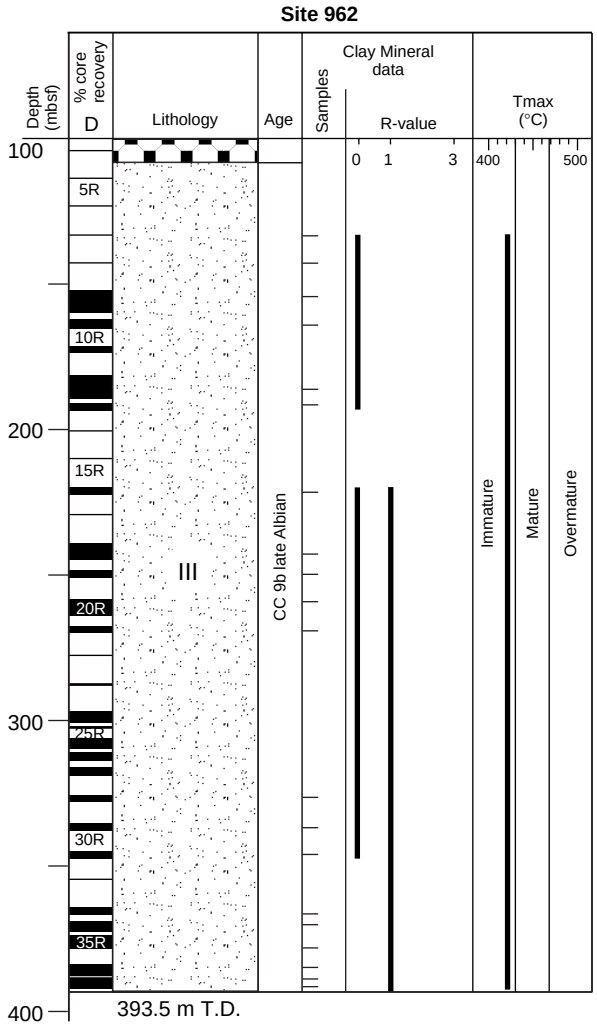

Figure 7. Summary of XRD data on the <0.5-µm-sized fraction from Hole 962D. CC9b refers to nannofossil biozone from Watkins et al. (Chap. 26, this volume). For key to lithologic symbols, see Figure 3. T_{max} data from Shipboard Scientific Party (1996d).

ed samples, dominates over the interval from 206.8 to 277.8 mbsf in Hole 961A (Fig. 10B), but disappears in deeper samples (Figs. 6, 10C). There is no notable lithologic variation in this interval that might account for this occurrence (Fig. 6; Shipboard Scientific Party, 1996d). Chlorite is present in most, but not all, samples. A trace of quartz occurs in several samples from Hole 961A, but in only two samples from Hole 961B.

Site 962

Recovery in Hole 962B was poor, and only drilling-induced breccia from the base of the mid-Cretaceous lithologic Subunit IIC was analyzed from this hole (Table 4). All samples contain R = 0 I/S clay and a trace of illite. Sample 159-962B-8H-5, 140–142 cm (71.9 mbsf), also contains palygorskite (see Pletsch, Chap. 15, this volume). Recovery was somewhat better in the deeper parts of Hole 962D, where coring began at 73.0 mbsf. R = 0 I/S clay dominates the upper six samples, from 133.3 to 191.4 mbsf (Figs. 7, 11A; Cores 159-962D-7R through 13R), all dated as nannofossil biozone CC9b, latest Albian to early Cenomanian (see Watkins et al., Chap. 26, this volume). Illite is also present, as indicated by asymmetrical peaks at both 10 and 5 Å (Fig. 11A). Kaolinite and/or chlorite are sporadically present in minor amounts (Table 4). Traces of both quartz and calcite occur in most of the samples, the latter arising from both calcite cement in sandier intervals, and partly dissolved nannofossils in the finer-grained samples. Cores 159-962D-14R through 15R had no or very little recovery, and beginning with Sample 159-962D-16R-2, 24–26 cm (221.7 mbsf), a mixture of both R = 1 and R = 0 I/S occurs, based on the presence of very broad peaks at both 17 and 13 Å in glycolated samples (Fig. 11B). The R = 0 I/S clay is a very minor component and its 002/003 peak could not be distinguished, but the R = 1 I/S clay has a range of 70%–85% illite layers in these samples. Minor components include illite, kaolinite, and chlorite, the latter in only two samples (Table 4). Traces of quartz and calcite are ubiquitous. A sampling gap occurs between 269.2 and 326.2 mbsf owing to poor recovery or recovery of only drilling rubble, but the next three samples, from Cores 159-962D-29R through 31R (326.2 to 345.9 mbsf), also contain a mixture of R = 0 and R = 1 I/S clay, similar to the overlying samples (Fig. 7). This interval is all within the CC9b nannofossil biozone (see Watkins et al., Chap. 26, this volume). Below this depth, in sediment of the same age, all samples contain R = 1 I/S clay, with a nonexpandable component ranging from 74% to 78% (Table 4; Figs. 7, 11C). Kaolinite and detrital illite are present in all samples; chlorite is present in only a few (Table 4). A trace of quartz occurs in two samples from 369.9 and 378.1 mbsf, a trace of calcite in one from 391.2 mbsf (Table 4).

DISCUSSION

Site 959

Detrital Clay Mineral Assemblage

R = 0 I/S clay dominates in samples from the lower part of the largely undisturbed lithologic Unit III (Table 1; Fig. 4). The proportion of nonexpandable clay varies from 5% to 30% and shows no regular increase with depth in this lithologic unit (Table 1; Fig. 4). These clay mineral data agree with an unpublished set of data on the <2-µm fraction over the same interval (T. Pletsch, pers. comm., 1996). These results suggest that the black siltstones and claystones of lithologic Unit III have not been subjected to temperatures much above 60°C (Pollastro, 1993). A 10-Å mineral is present in a few samples from this lithologic unit, but the absence of R = 1 I/S clay suggests that this mineral is detrital illite rather than a thermally induced, diagenetic R = 3 I/S or illite clay. The presence of nacrite veins in the black clay- and siltstones indicate the circulation of hydrothermal fluids. The interval with the nacrite veins is barren of biostratigraphic fossils, but is Late Cretaceous in age based on Maastrichtian dates above and early Santonian dates below (see Watkins et al., Chap. 26, this volume). The veins persist to the base of the hole, and suggest an emplacement date of pre-Maastrichtian, post-early Santonian.

R = 0 I/S clay becomes less expandable as it persists into the underlying lithologic Subunit IVA (Fig. 4). An abrupt transition occurs between Cores 159-959D-67R and 68R, with the upper core containing R = 0 I/S clay with 58% nonexpandable layers, and the lower core containing R = 1 I/S clay, with 76% nonexpandable layers. All samples below the first appearance of R = 1 I/S clay contain no R = 0 I/S clay, but do contain both R = 1 I/S clay and a mineral that is either R = 3 I/S clay or illite. The R = 3 I/S clay is indicated by the presence of a broad peak at 5 Å, which occurs in addition to the R = 1 I/S peak near 4.9 Å (Fig. 8C–E). The stratigraphic section that bears this transition from R = 0 I/S clay to R = 1 I/S clay may not be complete, how-

Table 1. XRD results of samples analyzed from Hole 959D.

Core, section, interval (cm)	Depth (mbsf)	Lith. unit	R, Smc	% Ill	Chlor	Ill	Kao	Others
159-959D-								
60R-5, 56-58	982.7	III	0	24		x		qtz
61R-2, 47-50	987.8	III	0			tr		calc
62R-1, 128-130	996.7	III	0	12		x		
63R-2, 56-58	1007.1	III	0	20		x		qtz, tr. plag
63R-6, 23-26	1012.7	III	0	30		x		qtz
64R-3, 48-50	1018.2	III	0	20	tr	x	tr	qtz
65R-2, 129-132	1026.9	III	0	5	tr	x		qtz, tr. calc, tr. k-spar
65R-6, 13-16	1031.7	III	0			x		qtz, calc
66R-6, 17-20	1041.4	III	0	20		tr		qtz, calc
67R-1, 118-121	1044.5	IVA	0	58		x	tr	tr. qtz
68R-1, 57-60	1053.6	IVA	1	76	x	x	x	tr. qtz, tr. calc
71R-1, 64-67	1082.3	V	1	62	x	x		
72R-4, 30-32	1096.0	V	1	77	x	x		tr. qtz
73R-1, 95-97	1101.8	V	1	82	x	x		
74R-2, 76-77	1112.8	V	1	70	x	x		
75R-1, 107-109	1121.3	V	1	78	x	x		
76R-2, 42-43	1131.7	V	1	80	x	x		
77R-1, 115-117	1140.7	V	1	80	x		tr	
78R-6, 60-62	1157.3	V	1	85	x	x	tr	

Note: Lith. Unit = Lithologic unit; R, Smc = Reichweite value of I/S clay; % Ill = % nonexpandable (illitic) layers in I/S clay; Chlor = chlorite; Ill = illite; Kao = kaolinite; qtz = quartz; calc = calcite; plag = plagioclase; k-spar = potassium feldspar; tr = trace; x = present.

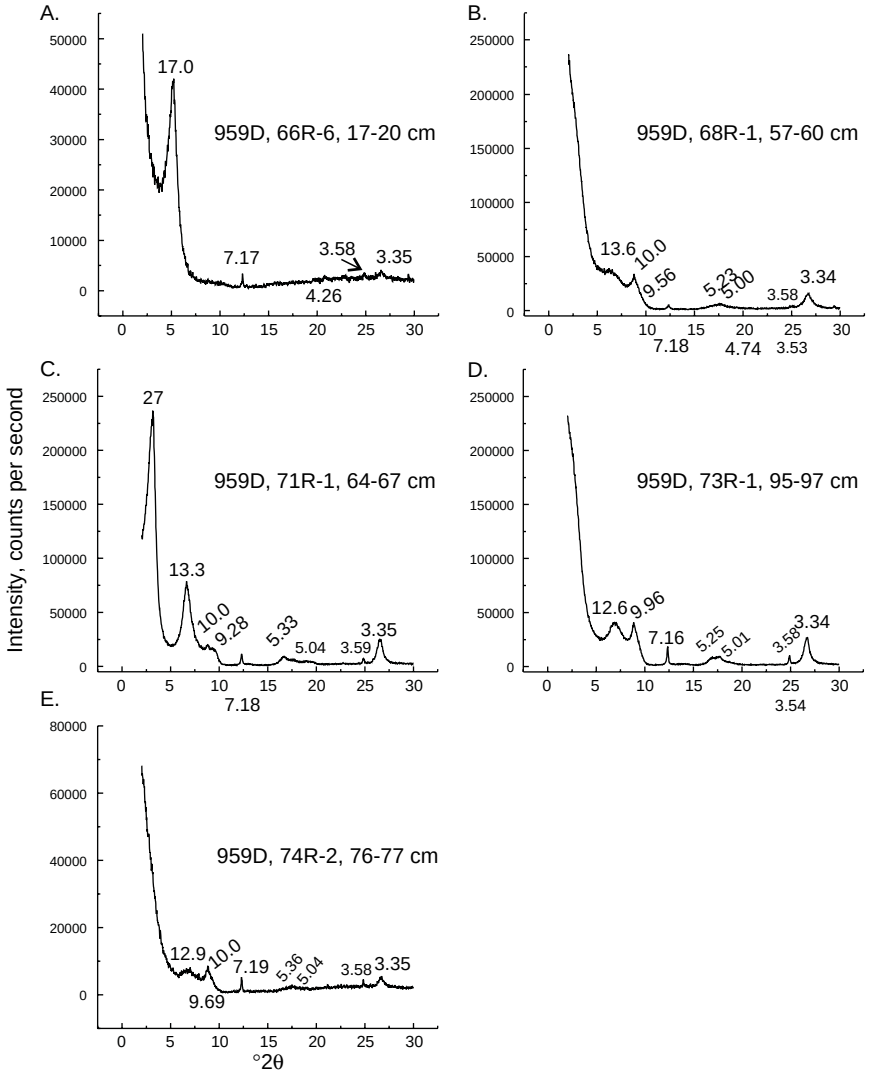

Figure 8. Selected X-ray diffractograms of <0.5-µm samples from Hole 959D, showing the change from randomly interstratified (R = 0 I/S) clay to regularly interstratified (R = 1 I/S) with depth. Numeric labels are d-spacings in angstroms. **A.** R = 0 I/S clay is indicated by a 17 Å peak. Kaolinite and a trace of quartz are also present. **B.** R = 1 I/S clay is indicated by a peak at 13 Å. 10 and 9.56 Å peaks were differentiated using profile fitting, as were peaks at 5.23 and 5.00 Å. **C.** The only sample analyzed with a superlattice peak at 27 Å. Peaks around 10 and 5 Å were differentiated using profile fitting. **D, E.** Peaks around 10 and 5 Å were differentiated using profile fitting.

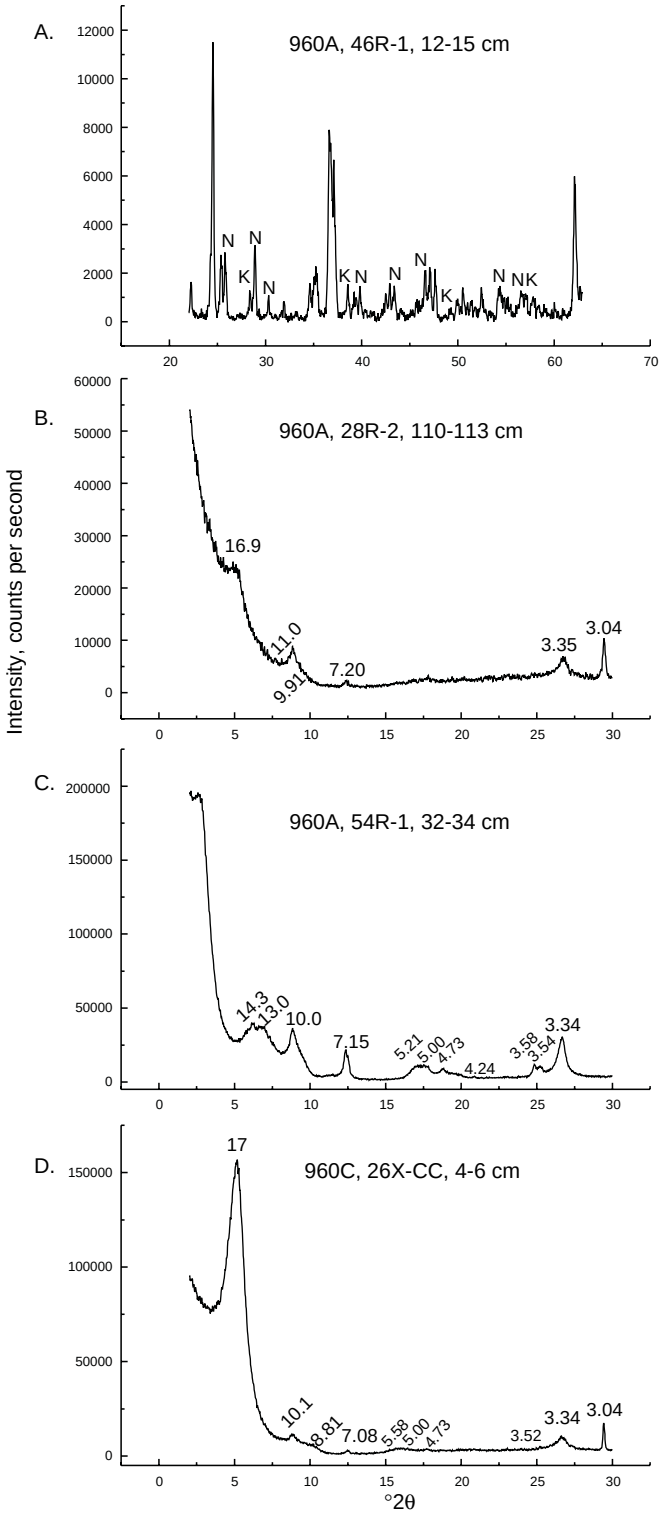

Figure 9. Selected X-ray diffractograms of the <0.5-µm-sized fraction of samples from Site 960. Numeric labels are d-spacings in angstroms. **A.** Randomly oriented sample picked from a kaolin vein. Diagnostic peaks for kaolinite and nacrite are shown. K = kaolinite; N = nacrite. **B.** Sample from lithologic Subunit IVB showing a probably detrital mixture of R = 0, R = 1, and R = 3 I/S clay, with kaolinite and calcite (3.04 Å). **C.** Thermally altered clay with a mixture of chlorite, R = 1 I/S clay, kaolinite, and a trace of quartz. **D.** Base of Hole 960C reached only to lithologic Subunit IVB, which is not affected by thermal diagenesis, as indicated by the R = 0 I/S clay at 17 Å.

Table 2. XRD results of samples analyzed from Site 960.

Core, section, interval (cm)	Depth (mbsf)	Lith. Unit	R, Smc	% Ill	Chlor	Ill	Kao	Others
159-960A-								
20R-1, 48-50	175.0	III						
28R-2, 110-113	253.9	IVB	0, 3			x	x	calc; k-spar
29R-2, 63-67	257.7	IVB	0			x	tr	calc
37R-1, 55-58	329.1	VA	0, 1			x	x	
37R-1, 71-73	329.2	VA	0,1			x		
38R-1, 113-116	339.3	VA	1		x	x	x	
40R-1, 23-25	348.5	VA	3		x			
41R-2, 04-06	352.5	VA	1		x	x	x	
42R-1, 34-36	353.8	VA	1		x	x	x	
43R-1, 47-49	358.0	VA	1		x	x	x	
44R-2, 35-38	364.2	VA	1		x	x	tr	tr. qtz
45R-1, 117-119	368.4	VA	1		x	x		
46R-1, 12-15	371.9	VA	1		x	x		
47R-1, 58-60	377.4	VA	1			x	tr	
48R-1, 74-78	380.0	VA	1		x	x	tr	tr. qtz
49R-1, 11-13	386.5	VA	1		x	x		
50R-1, 19-21	391.3	VA	1		x	x	x	
52R-1, 109-111	398.4	VA	1		x	x	tr	
53R-1, 39-41	403.7	VA	1		x	x	x	
54R-1, 32-34	413.4	VB	1,3		x	x	x	
55R-1, 24-26	418.0	VB	1,3		x	x	x	
56R-1, 70-74	423.5	VB	1		x	x	x	
57R-1, 84-89	428.2	VB	1,3		x	x		
58R-1, 67-69	433.1	VB	1		x	x	tr	
59R-1, 28-30	437.3	VB	1		x	x	tr	
60R-1, 61-64	442.6	VB	1		x	x		
61R-1, 17-19	446.4	VB	1		x	x		
159-960C								
13H-CC, 14-16	120.4	IIA	0			tr	x	
15H-7, 9-11	138.8	IIA					tr	
17X-CC, 7-9	142.0	IIA	0			tr		calc
21X-CC, 22-24	179.2	III						paly
22X-1, 35-37	189.0	III						paly
26X-CC, 4-6	346.0	IVB	0	25		x	tr	tr. calc; qtz

Note: For explanation of abbreviations, see note for Table 1.

ever, as both Cores 159-959D-67R and 68R had poor recovery. The apparently abrupt transition from R = 0 I/S clay to R = 1 I/S clay may be an artifact of erosion if there is an unconformity within this interval.

The next downhole sample, 159-959D-71R-1, 64–67 cm (1082.3 mbsf), is the only one from this site which exhibits the 27 Å superlattice peak (Fig. 8C). The sample from Core 159-959D-68R appears out of place in the downhole sequence because it has no superlattice peak and it contains a higher proportion of nonexpandable layers (thus indicating it reached a higher paleotemperature) than those in the underlying sample from Core 159-959D-71R (Fig. 4). Nannofossil evidence from Core 159-959D-68R indicates latest Albian–Cenomanian nannofossils have been reworked into an early Turonian assemblage (see Watkins et al., Chap. 26, this volume). This suggests that the clay in Core 159-959D-68R may be detrital, that is, reworked as the nannofossils were, during the Turonian, from thermally altered Albian–Cenomanian sediment. They are probably not an in situ diagenetic product. That Site 959 would for a time receive only thermally altered sediment, with no input of "fresh," expandable clay, is in fact not surprising when its location is viewed on seismic line MT02 (Fig. 12). Site 959 occurs on the side of a tectonically disturbed, and probably thermally altered (cf. results from Site 960), submarine, topographically elevated feature. The sediment of lithologic Unit IV is redeposited from shallow water reef and siliciclastic terranes to the south (i.e., the top of the submarine feature; see Marcano et al., Chap. 8, this volume). In addition, depositional rates for this unit are exceedingly low, on the order of millimeters per millions of years. (D. K. Watkins, pers. comm., 1996). The transition from R = 1 I/S clay to R = 0 I/S clay within this lithologic unit is probably a result of a change in provenance rather than a thermally induced transition.

Thermally Altered (Diagenetic) Clay Mineral Assemblage

All of the samples from lithologic Unit V, including those from the lithologically anomalous Core 159-959D-71R, are predominantly

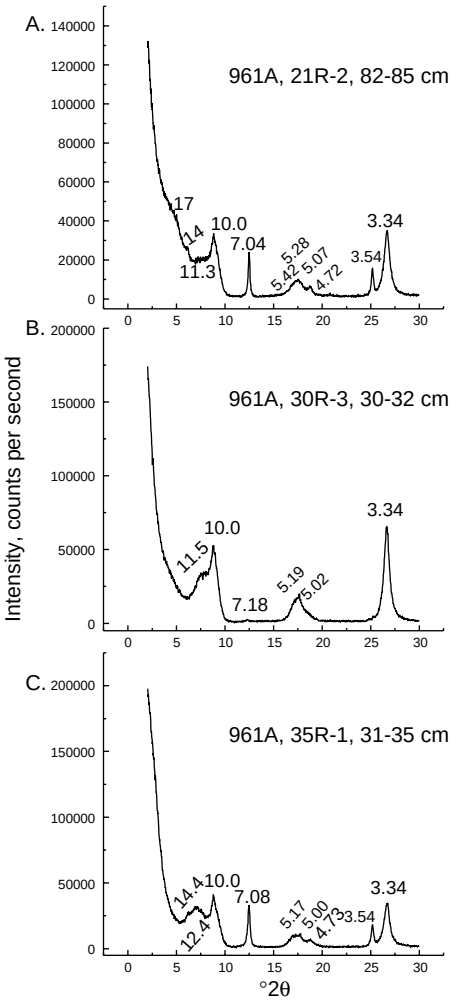

Figure 10. Selected X-ray diffractograms of the <0.5-µm-sized fraction of samples from Hole 961A showing the change from (**A**) R = 0 I/S clay, to (**B**) R = 3 I/S clay, to (**C**) R = 1 I/S clay. The middle interval with dominant R = 3 I/S clay may be a fault block, or all of these samples may represent a detrital mix of clays. Numeric labels are d-spacings in angstroms.

R = 1 I/S clay, with small amounts of R = 3 I/S clay or illite. The clay shows a slight increase in nonexpandability with depth (Fig. 4), and there is a change from R = 1 I/S clay showing a superlattice peak to I/S clay without such a peak (Fig. 8A–E). No biostratigraphically useful fossils were recovered from this unit, and it has no date (Shipboard Scientific Party, 1996b; see Watkins et al., Chap. 26; see Oboh-Ikuenobe et al., Chap. 25; both this volume). Thus, sediment that could be dated with nannofossils appears to be unaffected by a heating event, while older and undatable sediment does appear affected by a heating event. How hot was this heating event?

Most R = 0 I/S clay disappears at temperatures of around 100°C in basins with normal geothermal gradients, but at 120°C in younger basins with a high geothermal gradient or those that were subjected to hydrothermal activity (Pollastro, 1993). If heating were caused by burial of this sediment in a basin with a normal geothermal gradient (e.g., 15°–30°C/km), then burial depths of 7 to 4 km, respectively, would be required to raise the temperature to 100°C, and some 6 to 3 km of sediment would have been removed by erosion prior to deposition of the thermally unaltered mid-Upper Cretaceous section (lithologic Unit IV). This seems an unreasonably great depth. Based on dredge samples and seismic interpretations, Mascle and others (1996) estimated 1 km of uplift for the marginal ridge. It seems more reasonable to presume a somewhat higher paleogeothermal gradient than "normal" for Site 959 prior to the latest Albian. Assuming an elevated paleogeothermal gradient, the lower limit for the paleotemperature of the sediment in Core 159-959D-71R and deeper can be further constrained from 100°–120°C to around 120°C. An upper limit is around 170°C, as indicated by the absence of R = 3 I/S clay (Pollastro, 1993). The heating of lithologic Unit V occurred prior to latest Albian–early Cenomanian (Fig. 4).

Table 3. XRD results of samples analyzed from Site 961.

Core, section, interval (cm)	Depth (mbsf)	Lith. Unit	R,Smc	% Ill	Chlor	Ill	Kao	Others
159-961A-								
21R-2, 82-85	189.0	III	0, 3, 1		x	x		tr. qtz
22R-1, 113-115	197.5	III	1, 3		x			tr. qtz
23R-1, 72-74	206.8	III	3, 1		x			tr. qtz
24R-1, 140-142	217.1	III	3, 1		x			tr. qtz
25R-2, 40-42	227.4	III	3, 1		x			
26R-1, 131-133	236.9	III	3, 1		x			tr. qtz
27R-1, 44-46	246.1	III	3, 1		x			
28R-2, 32-34	257.1	III	3		x			
29R-1, 109-111	266.0	III	3					
30R-3, 30-32	277.8	III	3		tr			
31R-1, 113-115	285.3	III	1		x	x		
32R-1, 29-32	294.1	III	1		x	x		tr. qtz
33R-1, 27-29	299.8	III	1		x			
34R-1, 52-54	304.0	III	1		x			tr. qtz
35R-1, 31-35	308.5	III	1		x			tr. qtz
159-961B-								
2R-2, 16-18	227.7	III						
3R-2, 50-52	238.0	III	1		x	x		
4R-3, 137-140	264.3	III	1			x		
5R-2, 137-140	270.4	III	1		x	x		
6R-1, 35-36	274.9	III	1		x	x		
6R-2, 30-34	276.3	III	1		x	x		
7R-1, 52-54	284.7	III	1		x	x		tr. qtz
8R-2, 91-93	296.2	III	1		x	x		tr. qtz
10R-4, 46-50	313.7	III	1		x	x		
11R-1, 78-80	318.2	III	1		x	x		
12R-1, 23-26	322.6	III	1		x	x		
13R-2, 29-30	333.9	III	1		x	x		
15R-2, 98-99	353.9	III	1		x	x		
16R-2, 102-105	358.2	III	1		x	x		
17R-1, 51-53	361.2	III	1		x	x		tr. qtz
18R-2, 56-60	364.6	III	1		x	x		

Note: For explanation of abbreviations, see note for Table 1.

Table 4. XRD results of samples analyzed from Site 962.

Core, section, interval (cm)	Depth (mbsf)	Lith. Unit	R,Smc	%Ill	Chlor	Ill	Kao	Others
159-962B-								
8H-5, 140-142	71.9	IIC	0			x		paly
9H-3, 20-22	77.2	IIC	0			tr		
9H-6, 21-23	81.7	IIC	0			tr		
159-962D-								
7R-1, 27-28	133.3	III	0					
8R-CC, 6-8	142.8	III	0		x			
9R-2, 20-22	154.1	III	0	30		x	x	
10R-2, 51-53	164.0	III	0					
12R-4, 27-29	186.1	III	0	30		x	x	qtz, calc
13R-1, 43-45	191.4	III	0			x		calc, qtz
16R-2, 24-26	221.7	III	0,1	72		x	x	qtz, calc
18R-3, 74-76	242.8	III	0,1	76	x	x	x	qtz
19R-1, 98-100	249.8	III	0,1	83	x	x	x	qtz
20R-1,81-84	259.2	III	0,1	63		x	x	qtz, tr. calc
21R-1, 117-119	269.2	III	0			x	x	qtz, tr. calc
29R-1, 18-20	326.2	III	1,0	72		x	x	tr. calc, qtz
30R-1, 113-115	336.7	III	0,1			x	x	tr. calc
31R-1, 60-62	345.9	III	1	80	tr	x	x	tr. calc, qtz
33R-2, 19-21	366.2	III	1	74		x	x	
35R-3, 80-82	378.1	III	1	76		x	x	qtz
36R-1, 102-103	384.9	III	1	78		x	x	
37R-1, 17-19	388.7	III	1	78		x	x	
37R-2, 117-120	391.2	III	1	78		x	x	tr. calc

Note: For explanation of abbreviations, see note for Table 1.

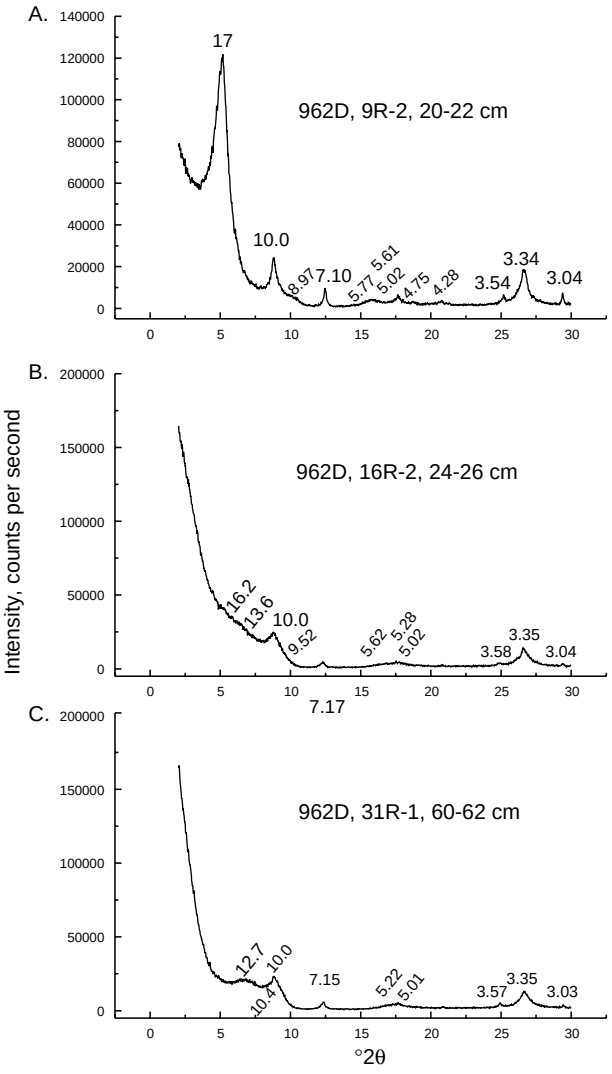

Figure 11. Selected X-ray diffractograms of the <0.5-µm-sized fraction of samples from Site 962 showing transition from (**A**) R = 0 I/S clay, through a mixture of (**B**) R = 0 and R = 1 I/S clay, to (**C**) R = 1 I/S clay in sediment of the same age, nannofossil biozone CC9b. Numeric labels are d-spacings in angstroms.

Site 960

The results from Site 960 are rather straightforward. The younger, tectonically undisturbed lithologic Unit IV of late Turonian to late Coniacian age contains predominantly R = 0 I/S clay, with some illite (Fig. 5). The presence of R = 0 I/S clay indicates that the temperature of this sediment never exceeded 100°C (Pollastro, 1993). The older, tectonically deformed and undated unit (Unit V), comprising an overlying shallow marine and an underlying lacustrine subunit, contains predominantly R = 1 I/S clay, with traces of R = 3 I/S clay in the upper part of the lacustrine subunit. Chlorite, illite, kaolinite, and quartz are ubiquitous, but no R = 0 I/S clay was observed. This clay mineral assemblage indicates that lithologic Unit V was affected by a heating event. The only exception for lithologic Unit V are the samples from the drilling-disturbed mud at the contact between this and the overlying lithologic Unit IV. These samples from Core 159-960A-37R contain a mixture of R = 0 and R = 1 I/S clay (Table 2). Unlike the underlying samples, these contain no chlorite or quartz, and do contain calcite. Considering the state of the core, this assemblage is probably drilling induced and represents downhole contamination from the overlying, non-altered unit (Pl. 3, Fig. 2).

The assemblage from Core 159-960A-38R to the base of the hole (lithologic Unit V) is interpreted as a product of thermal diagenesis of an unknown detrital assemblage, based on the absence of R = 0 I/S clay. The presence of R = 1 I/S with intermittent traces of R = 3 I/S clay suggests that the temperature of this sediment exceeded 100°–120°C, and may have just reached the threshold for the formation of R = 3 I/S clay, which is 170°–180°C (Pollastro, 1993). The chlorite polytype identified in these samples, IA or IB, ($\beta = 90°$), sometimes transforms to the IIB polytype at 150–200°C (Hayes, 1970), suggesting that the paleotemperature of lithologic Unit V was below this range. However, chlorite composition, oxygen fugacity, and pH of circulating fluids all influence the temperature of this transition in as yet unquantifiable ways, rendering paleotemperature estimates based on chlorite polytypes rather questionable (de Caritat et al., 1993).

Shipboard T_{max} data from lithologic Unit V suggests a paleotemperature in excess of 150°C (Fig. 5; Shipboard Scientific Party, 1996c; T. Wagner, pers. comm., 1995). It is unfortunate that no date could be obtained from lithologic Unit V, as the date of the heating event cannot be constrained except to say that it is pre-early Turonian. The presence of possibly detrital illite in lithologic Unit V precludes obtaining a radiometric age. If the clay and T_{max} signals indicating heating in the 150°–180°C range are correct, sediment heated to this paleotemperature is now resting at a burial depth of 340 m. A plot showing the temperatures 150° and 180°C at a depth of 340 m indicates a paleogeothermal gradient of 440°–530°C/km (Fig. 13). As this is rather high, and no analogous gradient could be found even for geothermal basins, it is reasonable to assume that this sediment was once buried deeper than it is today (i.e., that some sediment has been removed by erosion from Site 960, and that this erosion occurred after heating lithologic Unit V and prior to deposition of lithologic Unit IV).

Velde and others (1986) examined the clay mineral composition of sediment over a 2.5-km-thick interval in a borehole from the nearby Niger delta. The present day geothermal gradient there is around 80°C/km due to an intrusion to the southeast. Based on clay mineral and vitrinite reflectance data from sediment in the borehole, they estimated that the paleogeothermal gradient was 100°C/km. Their data could not constrain when this higher gradient existed. A similar paleogeothermal gradient for Site 960 would require the removal of over 1 km of sediment, probably not an unreasonable amount. All things considered, it seems reasonable that the paleogeothermal gradient for Site 960 was high, at or above 100°C/km, and thus consistent with the presence of a nearby spreading center.

Site 961

All samples from Hole 961B contain R = 1 I/S clay, which would indicate that paleotemperatures probably exceeded 100°C, but not 170°C (Fig. 6; Pollastro, 1993). In the adjacent hole, 961A, R = 3 I/S clay dominates from 189.0 to 277.8 mbsf (Table 3), while R = 1 I/S clay dominates sediment below that (285.3–308.5 mbsf, Table 3). There is T_{max} data for one sample from each interval, and both indicate immature organic matter (Fig. 6). If these data are reliable, they suggest the clay is detrital and not altered by heat. In this case, a source terrane supplied R = 1 I/S clay to this site while immature organic matter was being added. For some time, R = 3 I/S clay was also supplied to Hole 961A, but the timing cannot be known without better age control. Alternatively, if something is amiss with the shipboard T_{max} data, there is the problem of more heated, R = 3 I/S-bearing sediment (>170°–180°C, Pollastro, 1993) overlying less heated, R = 1 I/S-bearing sediment in Hole 961A, but not Hole 961B (Fig. 6). One possible explanation, if these clays are diagenetically formed and not detrital, is that a reverse fault has put more heated sediment above less heated sediment, although no such fault is visible on seis-

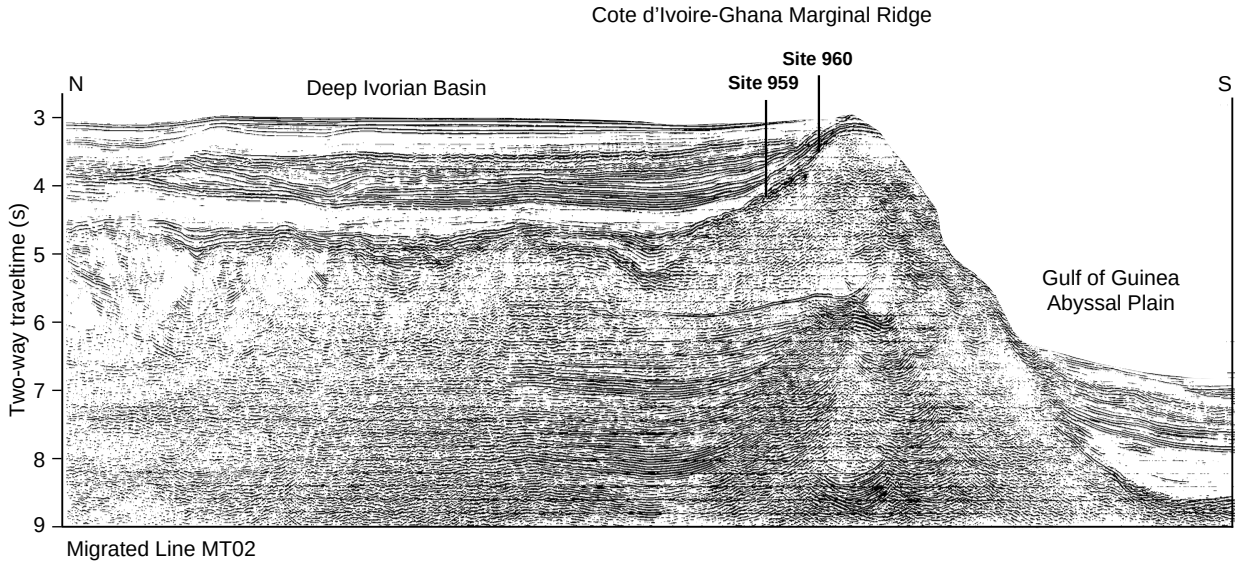

Figure 12. Seismic line MT02, showing relative positions of Sites 959 and 960 along a north-south transect. Site 959 was on the side of a submarine topographic high when the Deep Ivorian Basin first opened up. From Mascle et al. (1996).

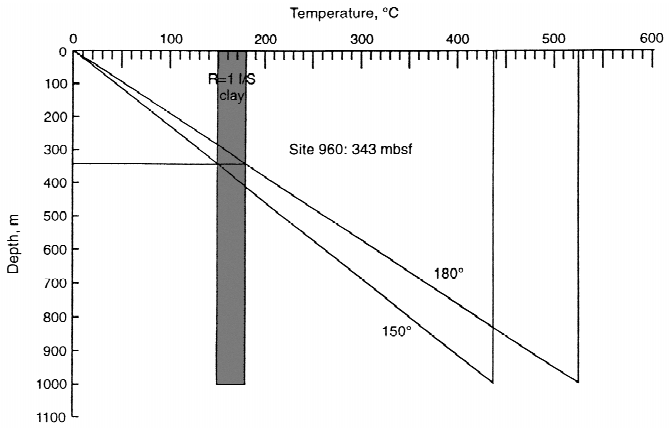

Figure 13. Possible paleogeothermal gradient for Site 960, based on paleotemperature estimates from clay mineral and T_{max} data. If the paleotemperature maximum was 150°C, the paleogeothermal gradient would have been nearly 440°C/km; if it were 180°C, the paleogeothermal gradient would have been around 520°C/km. As such high gradients are unlikely, some sediment has been removed by erosion from Site 960 following the thermal event and prior to deposition of lithologic Unit IVB, late Turonian–late Coniacian age.

mic sections over the area (Mascle et al., 1996). Alternatively, potassium may have been a limiting factor in R = 3 I/S clay formation over this interval. Since none of the sediment has any age control, results from this site can contribute nothing to our knowledge of the timing of tectonic events in this region. If the clays are diagenetic and not detrital, the same problems of an excessive paleogeothermal gradient as discussed for Site 960 could be overcome by citing erosion of several hundred meters of lithologic Unit III after it was heated, sometime prior to the Tertiary.

Site 962

Samples of latest Albian–Cenomanian age from the bottom of the hole all contain R = 1 I/S clay (Table 4; Fig. 7), suggesting these were either derived from a pre-heated terrane or were subjected to heating. Without an obvious lithologic break, they underlie samples of the same biozone (nannofossil biozone CC9b; see Watkins et al., Chap. 26, this volume) that contain a mixture of both R = 0 and R = 1 I/S clay. While these may represent a detrital mixture, it is not unreasonable to assume that they formed in a transition zone subject to heating above 60°C but not much above 100°C. Shipboard T_{max} values also indicate temperatures never exceeded approximately 100°C (Fig. 7; Shipboard Scientific Party, 1996e). This transitional interval, containing both R = 0 and R = 1 I/S clay, in turn underlies samples of the same age with only R = 0 I/S clay. All samples analyzed are derived from a single lithologic unit which has been folded, brecciated, and fractured, with fractures now filled by calcite and, in one zone, kaolin. It is remarkable that in nearly overturned beds in Core 159-962D-12R (Pl. 4, Fig. 3), R = 0 I/S clay, still highly expandable with only 30% nonexpandable layers, has survived the folding event. It indicates that folding at this site was post-latest Albian and was not necessarily associated with the thermal event.

The transition from R = 1 I/S clay at depth to the mixture of R = 0 and R = 1 I/S clay, to R = 0 I/S clay at shallower depths occurs over an interval of 175 m. Assuming a temperature of no more than 60°C for the R = 0 I/S clay at 191.9 mbsf, and a temperature of 120°–140°C for the R = 1 I/S clay at 366.2 mbsf, the paleogeothermal gradient would have been 343° to 457°C/km. The lower value is comparable to the highest gradient observed in the Buttes geothermal area of the southern, modern Salton Trough (Elders et al., 1972). The Salton Sea is in a pull-apart structure in a transitional tectonic regime between the East Pacific Rise plate boundary to the south and the San Andreas transform plate boundary to the north. The high geothermal gradient there is caused by a shallow intrusion of a basalt-rhyolite complex. This intrusion generated a hot brine diapir that rose to within 500 m of the surface (Elders et al., 1992). If the paleogeothermal gradient were like that of the modern Salton Sea, 350°C/km, then sediment would have to be buried to depths of 340–490 m to reach the temperatures necessary to react all R = 0 I/S clay and form R = 1 but not R = 3 I/S clay (i.e., 120°–170°C; assuming that K availability is not a limiting factor). This depth is now at 366.2 mbsf at Site 962 (Fig. 7). If indeed all of lithologic Unit III is one sediment package with no significant depositional breaks, as appears likely from the nannofossil ages, then 200 m of the sediment necessary to cause this degree of heating is still present, and less than 100 m of sediment has been lost

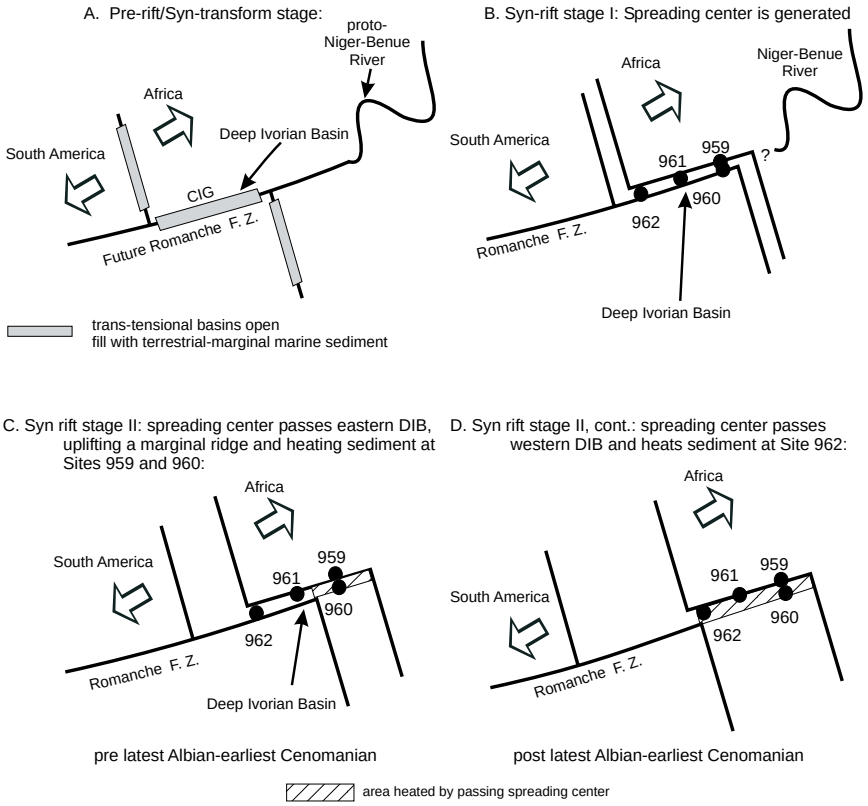

Figure 14. Summary illustration of the opening of the South Atlantic ocean along the Romanche Fracture Zone, and the formation of the Côte d'Ivoire-Ghana margin (CIG). **A.** As Africa and South America pull apart along the Romanche Fracture Zone, pull-apart basins, including the Deep Ivorian Basin, form. The proto Niger-Benue drainage system may have contributed sediment to this basin. **B.** The seafloor spreading center forms to the east of the Deep Ivorian Basin. **C**. The spreading center passes the eastern part of the basin, heating sediment (hatched area) at Sites 959 and 960. **D.** The spreading center passes the western part of the basin, heating sediment (hatched area) at Site 962.

by erosion from this site. The heating event occurred during or after the latest Albian–Cenomanian, and the erosion "event" was during the Late Cretaceous.

Timing of the Heating Event

Despite a frustrating lack of fossil preservation in the tectonically disturbed sediment recovered from the Côte d'Ivoire-Ghana margin during this leg, good biostratigraphic data from Sites 959 and 962 allow for some constraint on the timing of the thermal event, that is, the timing of the passage of the South Atlantic spreading center. The biostratigraphic and clay mineral data for Site 959 constrain the thermal event there to pre-nannofossil biozone CC9b, latest Albian to earliest Cenomanian, as sediment of this age is thermally unaltered and rests unconformably atop undated thermally altered sediment (Fig. 4; Table 1). Biostratigraphic and clay mineral data for Site 962 constrain the thermal event there to during or after nannofossil biozone CC9b, as sediment of that age contains diagenetic clay formed under elevated paleotemperatures (Fig. 7; Table 4). The newly formed South Atlantic spreading center thus passed along the Côte d'Ivoire-Ghana margin during nannofossil biozone CC9b during the latest Albian (Fig. 14).

SUMMARY AND CONCLUSIONS

The paleotemperature of the tectonically disturbed lithologic Unit V from Site 959 was 100°–180°C, based on the absence of R = 0 I/S clay, the dominance of R = 1 I/S clay, and the presence of R = 3 I/S clay in the <0.5-µm-sized fraction. This sediment is undated but unconformably underlies sediment of CC9b age, indicating that the thermal event which elevated sediment temperatures was pre-latest Albian–Cenomanian. The data also indicate that the paleogeothermal gradient was higher than "normal." Thermally altered sediment was the only detrital input into Site 959 during the initial emplacement of the mixed siliceous-carbonate clastics of lithologic Unit IV, following the thermal event. This lasted from the latest Albian to the early Turonian, a period of extremely low rates of deposition, after which thermally altered clay was no longer supplied to this site, but "fresh," thermally unaltered R = 0 I/S clay was.

The paleotemperature of tectonically disturbed sediment of lithologic Unit V at Site 960 reached 150°–180°C, based on the absence of R = 0 I/S clay, the dominance of R = 1 I/S clay, minor amounts of R = 3 I/S clay, and shipboard T_{max} data from organic matter. Paleogeothermal gradients were probably at least as high as they were at the nearby Niger Delta (100°C/km, Velde et al., 1986), otherwise an unreasonable amount of sediment would have to have been removed by erosion.

The results from Site 961 are highly problematic and may be due to their being a detrital, unheated assemblage, or the sequence studied was affected by a reverse fault cutting through this drill site. If heated, several hundred meters of thermally altered sediment were removed to account for the present depth; more would have been eroded given a lower paleogeothermal gradient. As there is no age control for the sediment at Site 961, more clear-cut clay mineral data would not have contributed any information to the timing of the thermal event at any rate.

At Site 962, the transition from thermally altered R = 1 I/S clay to unaltered R = 0 I/S clay occurs over a 175-m-thick interval. This indicates an intense, short-lived heating event during or after nannofossil biozone CC9b, in latest Albian–Cenomanian time. The reduced thickness of the transition zone suggests a very high paleogeothermal gradient, 340°–460°C/km. The lower value has a modern counterpart in the active geothermal Buttes area of the southern Salton Sea (Elders, et al., 1972). At this value, less than 100 m of sediment has been eroded from this site after the heating event and prior to deposition of the overlying Mn hardgrounds of probable Tertiary age (Shipboard Scientific Party, 1996e).

The passing of the South Atlantic spreading center may be age-constrained as follows: heating of undated sediment at Sites 959 and

960 was pre-latest Albian–Cenomanian (nannofossil biozone CC9b), and for Site 962 it was during or after the latest Albian–Cenomanian, indicating that the South Atlantic spreading center passed between Sites 959/960 and 962 during CC9b (Fig. 14). Folding of beds at Site 962 occurred during or after latest Albian–Cenomanian time, and may have occurred with uplift from the passing spreading center. Nacrite vein fill appears to be dissociated with the thermal event, as it occurs in unaltered sediment as young as post-early Santonian and pre-Maastrichtian. Barite veins are also not associated with the thermal event, as they occur in unaltered sediment as young as Maastrichtian. They may be associated with barite nodule formation in Eocene sediment (Shipboard Scientific Party, 1996c, 1996d, 1996e).

ACKNOWLEDGMENTS

Thanks very much to the crew of the *JOIDES Resolution* for hard work in hot conditions, and to a great group of ODP marine technicians, without whom these studies would not be possible. Thanks also to help in sample preparation from Mr. Kraig Heiden, Ms. Megan Cherry, Ms. Kelly Bergman, and Mr. Justin Spence. This paper was improved by stimulating discussions with all shipmates, particularly David Watkins, Kacey Lohmann, Thomas Pletsch, Tom Wagner, Franca Oboh, and Ken Hisada, but any errors are mine alone. Funding for this study was provided by the Joint Oceanographic Institutions/U.S. Science Advisory Committee.

REFERENCES

Biscaye, P.E., 1964. Distinction between kaolinite and chlorite in recent sediments by X-ray diffraction. *Am. Miner.*, 49:1281–1289.

de Caritat, P., Hutcheon, I., and Walshe, J. L., 1993. Chlorite geothermometry: a review. *Clays Clay Miner.*, 41:219–239.

Drever, J.I., 1973. The preparation of oriented clay mineral specimens for X-ray diffraction analysis by a filter-membrane peel technique. *Am. Mineral.*, 58:553–554.

Elders, W.A., McKibben, M.A., and Williams, A.E., 1992. The Salton Sea hydrothermal system, California, USA: a review. *In* Kharaka, Y.F., and Maest, A.S. (Eds.), *Proc. 7th Internat. Symp. on Water-Rock Interaction (Vol. 2): Moderate and High Temperature Environments.* Internat. Assoc. Geochem. Cosmochem. and Alberta Res. Council, 1283–1288.

Elders, W.A., Rex, R.W., Meidav, T., Robinson, P.T., and Biehler, S., 1972. Crustal spreading in southern California. *Science*, 178:15–24.

Elliott, W.C., and Matisoff, G., 1996. Evaluation of kinetic models for the smectite to illite transformation. *Clays Clay Miner.*, 44:77–87.

Eslinger, E., and Pevear, D., 1988. Clay minerals for petroleum geologists and engineers. *SEPM Short Course Notes*, 22.

Eslinger, E.V., Mayer, L.M., Durst, T.L., Hower, J., and Savin, S.M., 1973. An x-ray technique for distinguishing between detrital and secondary quartz in the fine-grained fraction of sedimentary rocks. *J. Sediment. Petrol.*, 43:540–543.

Hayes, J.B., 1970. Polytypism of chlorite in sedimentary rocks. *Clays Clay Miner.*, 18:285–306.

Hoffman, J., and Hower, J., 1979. Clay mineral assemblages as low grade metamorphic geothermometers: application to the thrust faulted Disturbed Belt of Montana, U.S.A. *In* Sholle, P.A., and Schluger, P.R. (Eds.), *Aspects of Diagenesis.* Spec. Publ.—Soc. Econ. Paleontol. Mineral., 26:55–79.

Jackson, M.L., 1975. *Soil Chemical Analysis—Advanced Course* (2nd ed., 10th printing): Madison, WI (Self-published).

Mascle, J., Lohmann, G.P., Clift, P.D., and Shipboard Scientific Party, 1996. Introduction. *In* Mascle, J., Lohmann, G.P., Clift, P.D., et al., *Proc. ODP, Init. Repts.*, 159: College Station, TX (Ocean Drilling Program), 5–16.

Moore, D.M., and Reynolds, R.C., Jr., 1989. *X-ray Diffraction and the Identification and Analysis of Clay Minerals:* Oxford (Oxford Univ. Press).

Pollastro, R.M., 1993. Considerations and applications of the illite/smectite geothermometer in hydrocarbon-bearing rocks of Miocene to Mississippian age. *Clays Clay Miner.*, 41:119–133.

Reynolds, R.C., Jr., 1980. Interstratified clay minerals. *In* Brindley, G.W., and Brown, G. (Eds.), *Crystal Structures of Clay Minerals and Their X-Ray Identification.* Mineral. Soc. London Monogr., 5:249–303.

————, 1985. *NEWMOD© a Computer Program for the Calculation of One-Dimensional Diffraction Patterns of Mixed-Layered Clays.* R.C. Reynolds, 8 Brook Rd., Hanover, NH.

Shipboard Scientific Party, 1996a. Principal results. *In* Mascle, J., Lohmann, G.P., Clift, P.D., et al., *Proc. ODP, Init. Repts.*, 159: College Station, TX (Ocean Drilling Program), 297–314.

————, 1996b. Site 959. *In* Mascle, J., Lohmann, G.P., Clift, P.D., et al., *Proc. ODP, Init. Repts.*, 159: College Station, TX (Ocean Drilling Program), 65–150.

————, 1996c. Site 960. *In* Mascle, J., Lohmann, G.P., Clift, P.D., et al., *Proc. ODP, Init. Repts.*, 159: College Station, TX (Ocean Drilling Program), 151–215.

————, 1996d. Site 961. *In* Mascle, J., Lohmann, G.P., Clift, P.D., et al., *Proc. ODP, Init. Repts.*, 159: College Station, TX (Ocean Drilling Program), 217–249.

————, 1996e. Site 962. *In* Mascle, J., Lohmann, G.P., Clift, P.D., et al., *Proc. ODP, Init. Repts.*, 159: College Station, TX (Ocean Drilling Program), 251–294.

Srodon, J., 1980. Precise identification of illite/smectite interstratifications by X-ray powder diffraction. *Clays Clay Miner.*, 28:401–411.

Velde, B., 1985. *Clay Minerals: A Physico-Chemical Explanation of Their Occurrence:* Amsterdam (Elsevier), *Dev. Sedimentol.*, 40.

Velde, B., Suzuki, T., and Nicot, E., 1986. Pressure-temperature-composition of illite/smectite mixed-layer minerals: Niger Delta mudstones and other examples. *Clays Clay Miner.*, 34:435–441.

Date of initial receipt: 17 September 1996
Date of acceptance: 27 May 1997
Ms 159SR-001

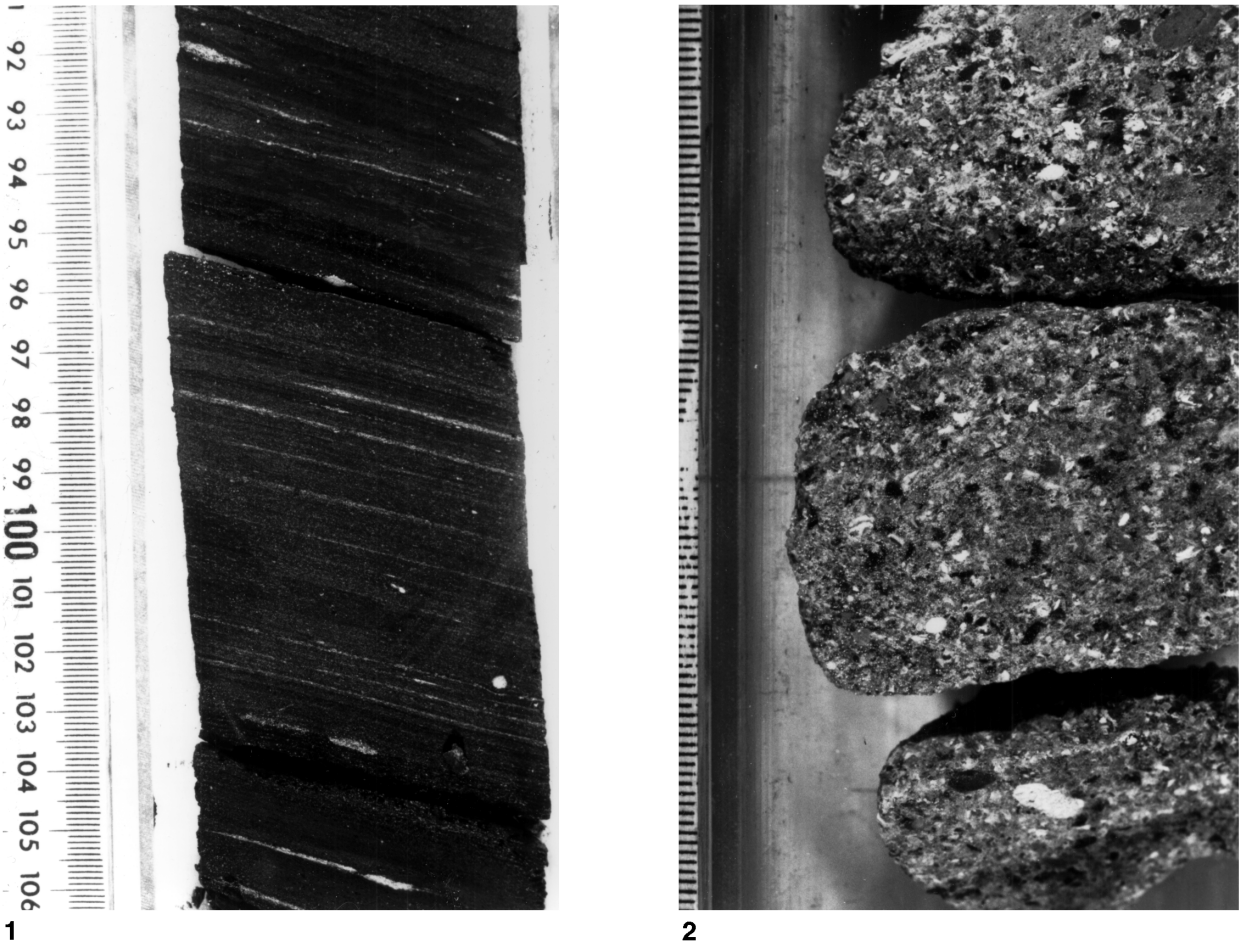

Plate 1. Core photographs of sediment from Hole 959D that was not heated much above 60°C, based on clay mineral data. **1.** Interval 159-959D-66R-6, 91–107 cm. Black clay- and siltstones of lithologic Unit III dip increasingly downhole. White streaks and blebs are pyrite-replaced burrows (the brassy luster reflects the light of the flash, appearing white) and thin laminae of replacement barite. **2.** Interval 159-959D-69R-1, 15–25 cm. Scale along left is in millimeters. Lithologic Subunit IVA, mixed siliceous-calcareous sediment.

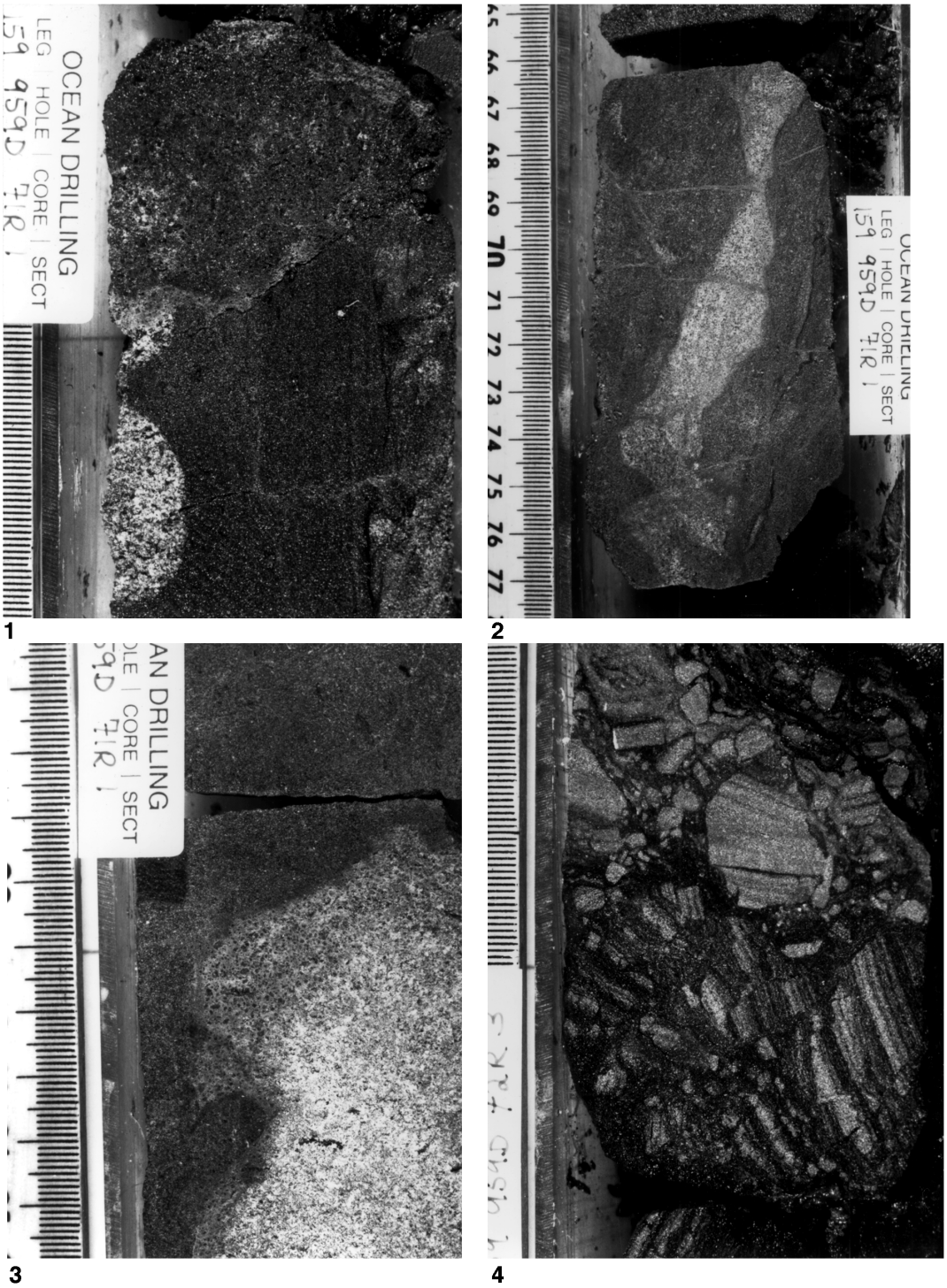

Plate 2. Photographs of core from thermally altered sediment (based on clay mineral data) at the base of Hole 959D. **1.** Interval 159-959D-71R-1, 40–55 cm. Coarse sandstone of lithologic Unit V, showing variation of lithology when compared to Figure 4. **2.** Interval 159-959D-71R-1, 65–78 cm. Coarse sandstone of lithologic Unit V, bearing a clastic dike which in turn is cut by clay-filled veins. **3.** Interval 159-959D-71R-1, 76–86 cm. Another clastic dike of very coarse sand into coarse sand, lithologic Unit V. **4.** Interval 159-959D-72R-3, 118–126 cm. Also lithologic Unit V, but a distinct lithology from that in Core 159-959D-71R. These sand- and siltstone laminae have been brecciated.

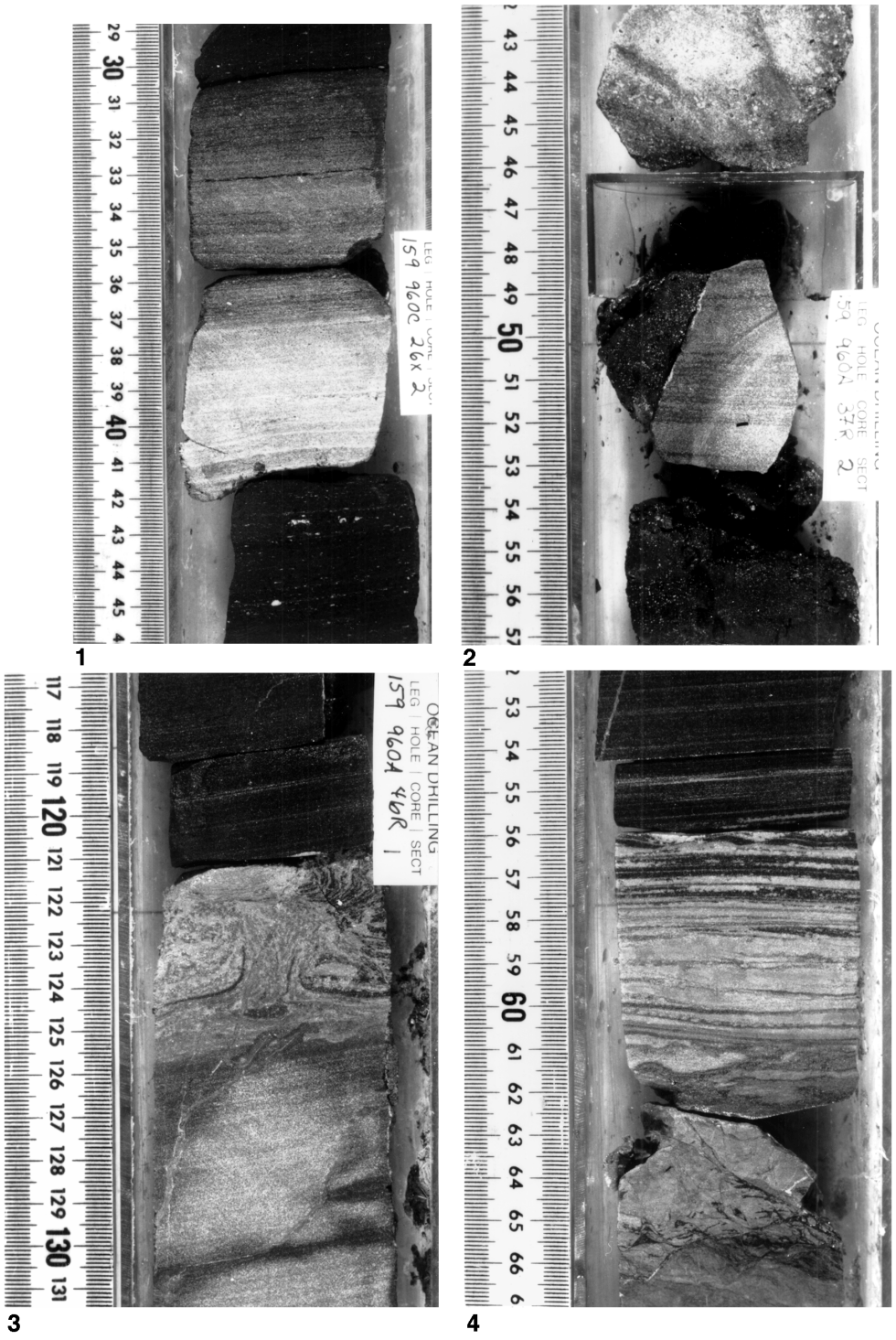

Plate 3. Photographs of sedimentary core from Site 960. **1.** Interval 159-960C-26X-2, 28–45 cm. Highly condensed Upper Cretaceous section of lithologic Subunit IVA. White blebs between 42 and 45 cm are barite nodules. The clay in this interval indicates that temperatures never exceeded ~60°C. **2.** Interval 159-969A-37R-2, 41–57 cm. Contact between mixed siliceous-carbonate sediment of lithologic Subunit IVB (41–46 cm) and lithologic Subunit VA (47–57 cm). The contact was disrupted by drilling. The soft mud between 47 and 57 cm has not been heated much above 60°C, and probably represents downhole contamination. **3.** Interval 159-960A-46R-1, 117–131 cm. Sand-, silt-, and claystones of thermally altered lithologic Subunit VA, showing syndepositional water-escape structure, 122–125 cm. **4.** Interval 159-960A-46R-2, 51–68 cm. Rippled laminae of shallow marine lithologic Subunit VA.

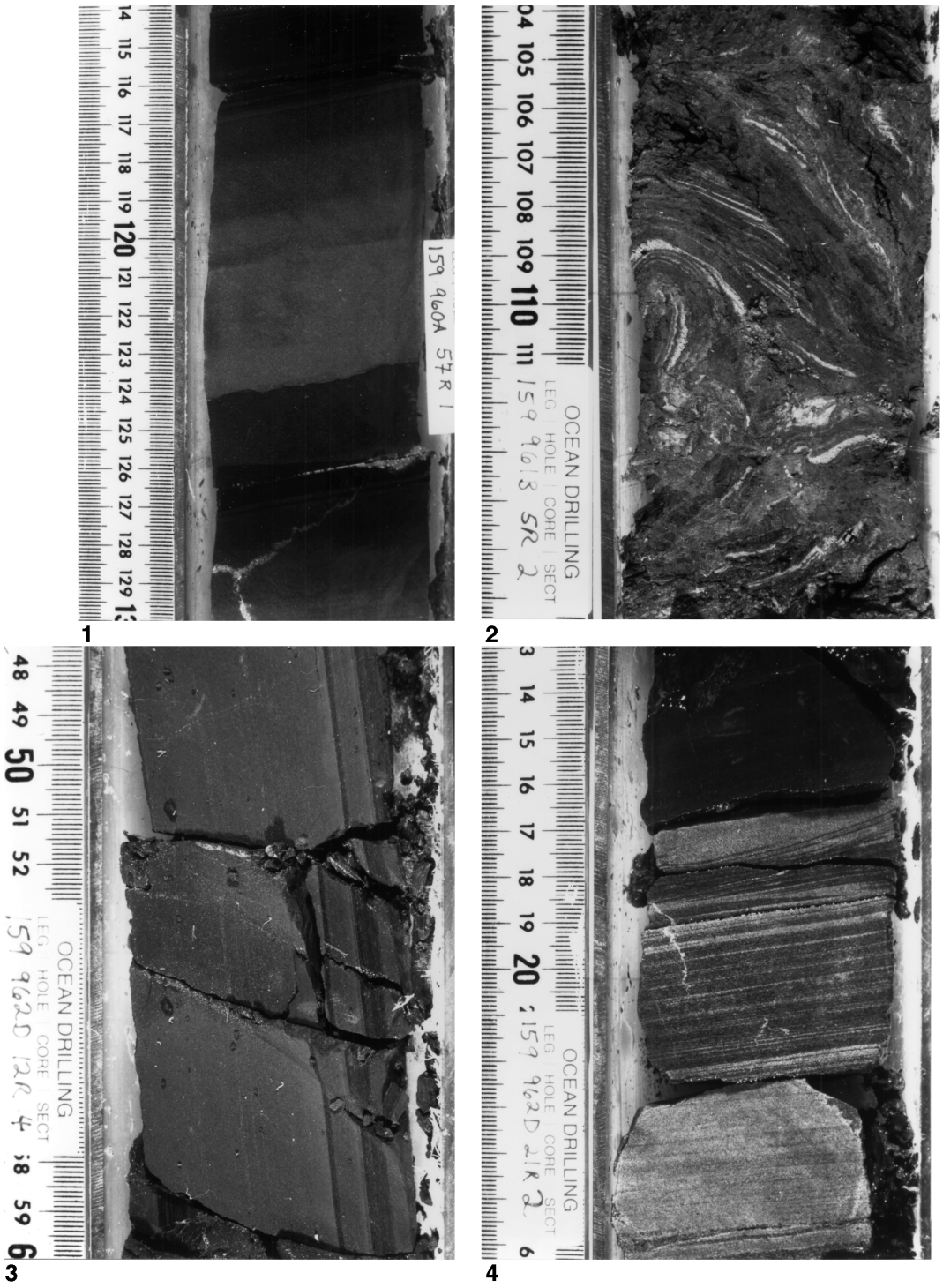

Plate 4. Photographs of sediment core from Sites 960–962. **1.** Interval 159-960A-57R-1, 113–130 cm. Turbidites in lacustrine sediment of lithologic Subunit VB. Graded bed with sole marks ranges from 121 to 124 cm. **2.** Interval 159-961B-5R-2, 103–117 cm. Thermally altered, tectonically disturbed, and poorly recovered sediment of lithologic Unit III. **3.** Interval 159-962D-12R-4, 47–60 cm. Near-vertical sand-siltstone strata of sediment from lithologic Unit III. This interval bears dominant randomly interstratified (R = 0) I/S clay, indicating temperatures have never exceeded 60°C. **4.** Interval 159-962D-21R-2, 13–27 cm. Sediment of lithologic Unit III that has been heated to 100–170°C, based on the co-occurrence of randomly (R = 0) and regularly (R = 1) interstratified I/S clay.